Title

Induced miR-99a expression represses Mtor cooperatively with miR-150 to promote regulatory T-cell differentiation

Journal

The EMBO Journal, 34(9)

ISSN

0261-4189

Authors

Warth, Sebastian C
Hoefig, Kai P
Hiekel, Anian
et al.

Publication Date

2015-05-05

DOI

10.15252/embj.201489589

Peer reviewed

Article

TRANSPARENT PROCESS

THE EMBO JOURNAL

Induced miR-99a expression represses *Mtor* cooperatively with miR-150 to promote regulatory T-cell differentiation

Sebastian C Warth[1], Kai P Hoefig[1], Anian Hiekel[1,†], Sonja Schallenberg[2], Ksenija Jovanovic[3,‡], Ludger Klein[3], Karsten Kretschmer[2], K Mark Ansel[4] & Vigo Heissmeyer[1,3,*]

Abstract

Peripheral induction of regulatory T (Treg) cells provides essential protection from inappropriate immune responses. CD4$^+$ T cells that lack endogenous miRNAs are impaired to differentiate into Treg cells, but the relevant miRNAs are unknown. We performed an overexpression screen with T-cell-expressed miRNAs in naive mouse CD4$^+$ T cells undergoing Treg differentiation. Among 130 candidates, the screen identified 29 miRNAs with a negative and 10 miRNAs with a positive effect. Testing reciprocal Th17 differentiation revealed specific functions for miR-100, miR-99a and miR-10b, since all of these promoted the Treg and inhibited the Th17 program without impacting on viability, proliferation and activation. miR-99a cooperated with miR-150 to repress the expression of the Th17-promoting factor mTOR. The comparably low expression of miR-99a was strongly increased by the Treg cell inducer "retinoic acid", and the abundantly expressed miR-150 could only repress *Mtor* in the presence of miR-99a. Our data suggest that induction of Treg cell differentiation is regulated by a miRNA network, which involves cooperation of constitutively expressed as well as inducible miRNAs.

Keywords miRNA function; T-cell differentiation; Treg cells
Subject Categories Immunology
DOI 10.15252/embj.201489589 | Received 22 July 2014 | Revised 19 December 2014 | Accepted 21 January 2015 | Published online 23 February 2015
The EMBO Journal (2015) 34: 1195–1213

See also: **A Liston & SM Schlenner** (May 2015)

Introduction

T helper cells can exert effector functions after activation and differentiation into Th1, Th2, Tfh and Th17 subsets. They can also control effector T cells as regulatory T cells (Treg). Treg cells express the lineage-specifying transcription factor forkhead box P3 (Foxp3) and suppress immune responses against self-antigens as well as against tolerated foreign antigens in mouse and man (Fontenot *et al*, 2003; Hori *et al*, 2003; Shevach & Thornton, 2014). Treg cells can develop in the thymus from single-positive CD4$^+$ thymocytes with an autoreactive T-cell receptor of moderate affinity (Jordan *et al*, 2001). They also differentiate in the periphery from naive T cells to generate tolerance to foreign antigens present in the food or in the air (Zhang *et al*, 2001; Chen *et al*, 2003; Kretschmer *et al*, 2005). Consequently, these peripheral regulatory T cells are of critical importance at mucosal surfaces but also contribute to feto-maternal tolerance (Josefowicz *et al*, 2012; Samstein *et al*, 2012). The differentiation of peripheral regulatory T cells can be recapitulated partially *in vitro* by stimulation of naive CD4$^+$ T cells via the T-cell receptor and the co-stimulatory receptor CD28 in the presence of TGFβ and IL-2 (Chen *et al*, 2003; Zheng *et al*, 2004). In contrast to Treg cells, Th17 cells have pro-inflammatory functions. They protect against bacterial and fungal infections and contribute to autoimmune disease. Th17 cell development is characterized by a high induction of the transcription factors RAR-related orphan receptor γt and α (RORγt and RORα) (Yang *et al*, 2008b). Similar to Treg cells, the *in vitro* induction of Th17 cells requires TGFβ, but additionally depends on the cytokine IL-6 (Bettelli *et al*, 2006; Veldhoen *et al*, 2006). The development of Treg and Th17 cells is reciprocally controlled, and the balance between the expression of transcription factors Foxp3 and RORγt/RORα is crucial in determining whether uncommitted CD4$^+$ T cells differentiate into the one or the other CD4$^+$ T-cell subset (Zhou *et al*, 2008a). Recent research has implicated differential usage of metabolism pathways in T cells into this lineage choice. While the dominant metabolic pathway during differentiation of effector T cells is aerobic glycolysis, lipid oxidation is preferentially employed to generate ATP in Treg cell differentiation. Mammalian target of rapamycin (mTOR) is a central regulator of aerobic glycolysis as well as a crucial negative regulator of Treg cell differentiation (Dang *et al*, 2011; Shi *et al*, 2011). Deletion of mTOR in T cells leads to a profound increase of Treg

1 Helmholtz Zentrum München, Research Unit Molecular Immune Regulation, Institute of Molecular Immunology, Munich, Germany
2 Molecular and Cellular Immunology/Immune Regulation, DFG-Center for Regenerative Therapies Dresden (CRTD), Technische Universität Dresden, Dresden, Germany
3 Institute for Immunology, University of Munich, Munich, Germany
4 Department of Microbiology and Immunology, University of California San Francisco, San Francisco, CA, USA
*Corresponding author. Tel: +49 89 2180 75629; E-mail: vigo.heissmeyer@med.uni-muenchen.de
†Present address: Gene Center, Department of Chemistry and Biochemistry, University of Munich, Munich, Germany
‡Present address: Department of General, Visceral, Transplantation and Thoracic Surgery, University Hospital of Munich, Munich, Germany

cell differentiation upon T-cell activation and completely abrogates Th17 cell differentiation. Therefore, mTOR can be considered a key regulator of reciprocal lineage choice. Finally, it has been shown that in cancer cells, which heavily rely on aerobic glycolysis, high mTOR expression is inversely correlated with the expression of several miRNAs, among them miR-99a and miR-100 (Torres *et al*, 2012).

The biogenesis of miRNAs produces ~22 nt long, double-stranded RNAs. Upon loading of a selected miRNA strand (i.e. the sense strand) into the RNA-induced silencing complex (RISC), the assembled miRISC functions as a *trans*-acting factor that identifies sequences in the 3′ UTRs of target genes. The miRISC-bound sequences are complementary to a 7–8 nt long sequence (i.e. the seed sequence) that starts with the second nucleotide at the 5′ end of the miRNA sense strand. Such target binding usually leads to translational inhibition and to the degradation of the transcript. On average, each miRNA has the potential to repress hundreds of transcripts, while mRNA 3′ UTRs can have up to several dozens of miRNA target sites. These sites are not randomly distributed but often occur in pairs or clusters, which can cooperatively repress mutual targets. The ideal distance for a cooperative miRNA effect was determined to have 13–35 nt between the recognized sites that are complementary to the seed sequences (Grimson *et al*, 2007; Sætrom *et al*, 2007; Broderick *et al*, 2011).

Ablation of miRNA biogenesis promotes Th1 differentiation but impairs Treg cell development (Muljo *et al*, 2005; Cobb *et al*, 2006; Chong *et al*, 2008; Steiner *et al*, 2011). Furthermore, impaired miRNA biogenesis in Foxp3$^+$ regulatory T cells causes severe spontaneous autoimmunity, highlighting the importance of miRNA expression in the maintenance of self-tolerance (Chong *et al*, 2008; Liston *et al*, 2008; Zhou *et al*, 2008b). However, it is currently unclear which miRNAs participate in the differentiation program of Treg cells. To address this issue, we performed an overexpression screen of miRNAs in naive CD4$^+$ T cells. We identified a large set of candidate miRNAs that promoted or interfered with Treg cell differentiation revealing an extensive early contribution of miRNAs in the establishment of T-cell fates. We selected miR-99a for further investigation, since this miRNA had a positive and specific impact on Treg cell differentiation. We showed that *Mtor*, a known inhibitor of Treg cell differentiation, is repressed not only by miR-99a, but also by the abundantly expressed miR-150 through an adjacent *cis*-element. Consistently, reducing cellular miR-150 expression with antagomirs reduced Treg cell differentiation *in vitro* and *in vivo*. The reconstitution of *Dicer*-deficient cells with miR-99a and/or miR-150 suggested a new mode of cooperation. In this mode, miR-99a, which is markedly induced after retinoic acid stimulation of T cells, strongly enhances target regulation by miR-150. Such a requirement for cooperation is encoded in the mRNA 3′ UTR and may confer a critical importance on particular miRNAs to direct cell fates even at moderate expression levels.

Results

An experimental window for miRNA regulation in Treg cell differentiation

miRNAs are critical for the differentiation of naive CD4$^+$ T cells into regulatory T cells (Cobb *et al*, 2006; Chong *et al*, 2008; Liston *et al*, 2008; Zhou *et al*, 2008b). We first determined when miRNAs can most effectively alter TGFβ-induced Treg cell differentiation (Chen *et al*, 2003; Zheng *et al*, 2004). Using flow cytometry, quantitative PCR and immunoblotting, we analyzed the timing of Foxp3 expression (Fig 1A–C). Intracellular Foxp3$^+$ staining was detected as early as 36 h after T-cell activation under Treg-polarizing conditions, which was consistent with a detectable rise in *Foxp3* mRNA and protein levels (Fig 1B and C). No further increase in the percentages of Treg cells was observed beyond the 48 h time point, at which time also the protein and mRNA levels approached their maximum (Fig 1A–C). Therefore, the instructive or modulatory effects of miRNAs on Treg cell differentiation that affect the initial expression of Foxp3 will operate within the first 36 h of stimulation.

We next analyzed the expression of Ago1-4 proteins, which are essential and limiting components of the RISC complex (Diederichs & Haber, 2007; O'Carroll *et al*, 2007; Bronevetsky *et al*, 2013). Interestingly, Ago1-4 protein expression, as detected by a pan-Ago antibody, was high in CD4$^+$ T cells during the first 36 h of Treg-polarizing conditions and decreased at 48–72 h after T-cell activation (Fig 1D). This finding is in line with previous experiments under Th1-polarizing conditions that suggested a general resetting of miRISC function due to proteasomal Ago1-4 degradation during Th1 differentiation (Bronevetsky *et al*, 2013).

Post-transcriptional gene regulation can also be modulated on the level of the miRNA-binding sites in target mRNAs. In activated CD4$^+$ T cells, many transcripts have shortened 3′ UTRs as a consequence of alternative splicing or alternative polyadenylation signal usage (Sandberg *et al*, 2008). This can lead to loss of distal regulatory elements of target mRNAs. Using transcriptome polyadenylation signal (PAS) mapping data from mouse brain, kidney, liver, muscle and testis (Derti *et al*, 2012), we looked for transcripts with 3′ UTR variants that correlated with the use of particular PAS. A marked example was the *Eri1* gene sequence which possesses at least five actively used PAS (Fig 1E and Supplementary Fig S1A). We designed two different qPCR assays that either amplified a sequence within the *Eri1* coding sequence (Fig 1E, CDS) or a sequence at the 3′ end of the 3′ UTR (Fig 1E, distal 3′ UTR). Quantifying PCR amplicons in the *Eri1* CDS, it became apparent that transcript levels stayed almost unchanged over a time-course of 72 h of T-cell activation under Treg-polarizing conditions (Fig 1F, left panel). In contrast, Eri1 protein levels steadily and strongly increased over the same period of time due to increased protein synthesis (Fig 1G), as we ruled out differential rates of Eri1 protein degradation in activated and resting T cells. Specifically, we showed that Eri1 protein levels in either naive or activated T cells were not affected by cycloheximide treatment for 1–6 h (Supplementary Fig S1D) at concentrations that effectively blocked *de novo* protein synthesis of CD25 and CD69 during the activation of naive T cells (Supplementary Fig S1E). We then asked whether the obvious disconnect between protein and mRNA abundance could be explained by the use of a more proximal PAS in the Eri1 gene to produce a shorter transcript that resulted in higher translation efficiency. To test this hypothesis, we quantified another PCR amplicon located directly upstream of the most distal PAS in the 3′ UTR of the *Eri1* mRNA (Fig 1F, right panel). Indeed, the abundance of this amplicon was strongly reduced (> 75%) as early as 12 h after T-cell activation and stayed low during the following 60 h of the experiment. The observed result is consistent with a switch to shorter

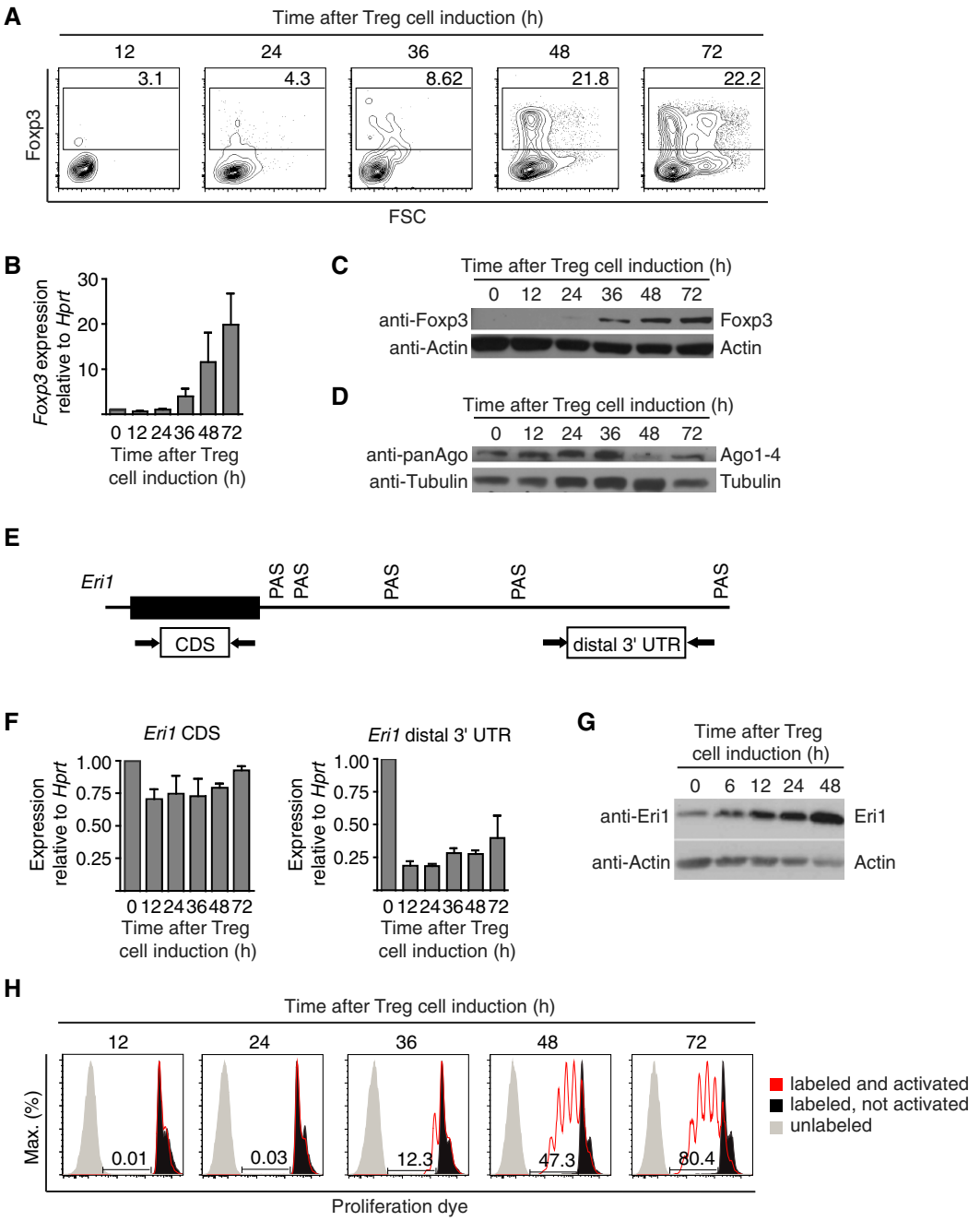

Figure 1. An experimental window for the regulation of Treg cell differentiation by miRNAs.

Naive CD4$^+$ T cells purified from Tg(DO11.10); Tg(CARΔ-1) mice were stimulated under Treg-polarizing conditions or left unstimulated and were analyzed at the indicated time points.

A Single-cell analysis of Foxp3 protein expression by intracellular anti-Foxp3 staining and flow cytometry.

B *Foxp3* mRNA levels were quantified using qPCR and normalized to the 0 h time point.

C, D Foxp3 protein (C) or protein expression of Ago proteins (Ago1-4) (D) were determined by immunoblotting with antibodies against Foxp3 or against all Argonaute proteins (panAgo).

E Schematic representation of the *Eri1* mRNA showing alternative polyadenylation signals (PAS) and primer pairs that were designed to detect the indicated amplicons within the *Eri1* coding sequence (CDS) or within the 3′ end of the *Eri1* 3′ UTR (distal 3′ UTR).

F *Eri1* mRNA variants were determined by qPCR using the primer pairs depicted in (E) after normalization to the 0 h time point.

G Expression of Eri1 protein was determined by immunoblotting.

H Proliferation was analyzed by labeling naive CD4$^+$ T cells with a proliferation dye prior to stimulation under Treg-polarizing conditions. Dilution of the proliferation dye was analyzed by flow cytometry. Unlabeled cells (gray areas) or unactivated cells (black areas) are shown as controls.

Data information: The data are representative of two or more independent experiments (A, C, D, G, H) or show means ± SD of two (F) or three (B) independent experiments.

Eri1 mRNA isoforms very early after T-cell activation under Treg-polarizing conditions. Differential PAS usage with similar kinetics was also detected when analyzing PCR amplicons positioned in the CDS and close to a PAS in the distal 3′ UTR of *Calm1* and *Tgfbr2* mRNAs, encoding two proteins that are important in TCR and TGFβ signaling in effector T cells and Treg cells (Liu, 2009; Sledzińska *et al*, 2013) (Supplementary Fig S1B and C, right panels). This regulation similarly occurred already 12 h after T-cell activation, but was not correlated with proliferation of cells that started with a first cell division around 36 h and reached four cell divisions between 48 and 72 h of stimulation (Fig 1H). Taken together, we propose a "window of opportunity" for testing miRNA-mediated repression during TGFβ-induced Treg cell differentiation. This experimental window ends after 36 h with the onset of Foxp3 expression. Furthermore, our analysis suggests that miRNA-mediated repression might be most effective early during T-cell activation before regulatory processes, such as Argonaute protein degradation or 3′ UTR shortening, can diminish its impact.

A forward screen to identify miRNAs that regulate Treg cell differentiation

Different miRNAs may act together in target regulation and may also have redundant effects. To assess the function of single miRNAs, we pursued a forward genetics approach in the context of endogenous miRNA expression. To be able to screen for effects of miRNAs on Treg cell differentiation, we set up a protocol of adenoviral transduction of pri-miRNAs into naive T cells (Warth & Heissmeyer, 2013). We used T cells from Tg(DO11.10); Tg(CARΔ-1) mice that are susceptible to adenovirus infection due to transgenic expression of a signaling-defective version (CARΔ-1) of the coxsackie adenovirus receptor (Wan *et al*, 2000). The mature miRNAs were processed from transcripts of vector-encoded "pri"-miRNAs, which were cloned as ~500 nt long stretches that included pre- and mature miRNA sequences (Chen *et al*, 2004). Resting the cells for 40 h in the absence of cytokines prior to activation under Treg-polarizing conditions (Fig 2A) enabled high levels of ectopic miRNA expression in naive $CD4^+$ T cells (Warth & Heissmeyer, 2013). Importantly, the transduction itself did not cause or affect T-cell activation and did not alter Treg cell differentiation (Warth & Heissmeyer, 2013). We set up a flow cytometry-based screen to measure miRNA regulation of Treg cell differentiation. miRNA sequences were cloned into IRES-GFP-containing constructs so that GFP expression could be used as a marker for T-cell infection in combination with intracellular Foxp3 expression that served as a marker for Treg cell differentiation. Both markers were then used to calculate "relative differentiation" for viable cells, that is, the ratio of differentiation in infected cells ($Foxp3^+$; GFP^+ divided by all GFP^+ cells) relative to the differentiation in non-infected cells ($Foxp3^+$;GFP^- divided by all GFP^- cells). By calculating the relative differentiation, we intrinsically controlled for varying transduction efficiencies. Relative differentiation was also found to be a robust measure for effects of the same construct in several cell culture wells that differed in their overall frequency of Treg cell differentiation.

To determine the dynamic range of the system, we ectopically expressed transcription factors that potentially promoted or repressed Treg cell differentiation. As Foxp3 is necessary and sufficient to establish Treg cell identity (Fontenot *et al*, 2003; Hori *et al*, 2003), we adenovirally transduced naive $CD4^+$ T cells with a construct expressing human FOXP3. After resting and subsequent activation under Treg-polarizing conditions for 72 h, Treg cell differentiation and endogenous Foxp3 expression were analyzed using a monoclonal anti-mouse Foxp3 antibody, which did not recognize epitopes of human FOXP3. Indeed, adenoviral FOXP3 overexpression doubled the relative Treg cell differentiation (Fig 2B). The transcription factor Foxp3 binds cooperatively with NFAT to composite binding sites, while NFAT is similarly able to cooperate with AP1 on the very same binding sites (Wu *et al*, 2006). Since NFAT/Foxp3 cooperation is required for Treg cell function (Wu *et al*, 2006), we inferred that overexpression of AP1 could potentially repress Treg-specific transcription. We adenovirally transduced naive $CD4^+$ T cells with a construct encoding *cJun* linked with a "self-cleaving" P2A sequence to *cFos* to obtain stoichiometric amounts of both components that can then heterodimerize and form the AP1 transcription factor. After 40 h resting and 72 h activation of the T cells under Treg-polarizing conditions, we detected massively reduced Treg cell differentiation (fivefold) in AP1-transduced cells (Fig 2C). These results indicated an overall dynamic range of the screening protocol of at least tenfold.

Biologically relevant repression is unlikely to be caused by miRNAs of low abundance; however, many miRNAs including well-studied drivers of cellular differentiation are upregulated in a confined spatial or temporal order. To select miRNA candidates for our screening library, we reviewed array-based and next-generation sequencing-based miRNA profiling data of various T-cell lineages and developmental stages, including Treg cells (Monticelli *et al*, 2005; Landgraf *et al*, 2007; Steiner *et al*, 2011; Thomas *et al*, 2012). From these data, miRNAs were chosen that showed medium to high abundance, even if their expression was restricted to a certain T-cell lineage or developmental stage. Eventually, we cloned 130 "pri"-miRNA fragments (Supplementary Table S1 and Supplementary Materials) from C57BL/6 genomic DNA into the pCAGAdDu-GFP vector (Warth & Heissmeyer, 2013) and generated a library based on 108 adenoviral constructs that encode individual or clustered miRNAs. Using this library, we performed a parallel overexpression screen for functional miRNAs in Treg cell differentiation (Fig 2D). Fifteen GFP-expressing control viral replicates, distributed at random positions over the screening plates, served to calculate the mean of the relative differentiation and the standard deviation ($RD = 1.006 \pm 0.06$) (Fig 2E). If the expression of a miRNA was able to shift the RD of regulatory T cells by more than twofold of the standard deviation, we considered the effect significant. In total, we identified 21 constructs with 29 miRNAs that inhibited and nine constructs with 10 miRNAs that promoted the differentiation of regulatory T cells. The strongest negative impact resulted from miR-193 expression, while miR-10b strongly enhanced Treg cell development (Fig 2D upper and lower panels).

Among the identified negative regulators miR-31 and miR-17~19a stood out. Consistent with the screening results, miR-31 is a known repressor of Foxp3 expression in human Treg cells (Rouas *et al*, 2009), and the miR-17~92 cluster has already been demonstrated to repress Treg cell formation and to promote effector T-cell differentiation into Th17 as well as Tfh subsets (Jiang *et al*, 2011; Baumjohann *et al*, 2013; Kang *et al*, 2013; Liu *et al*, 2014). The

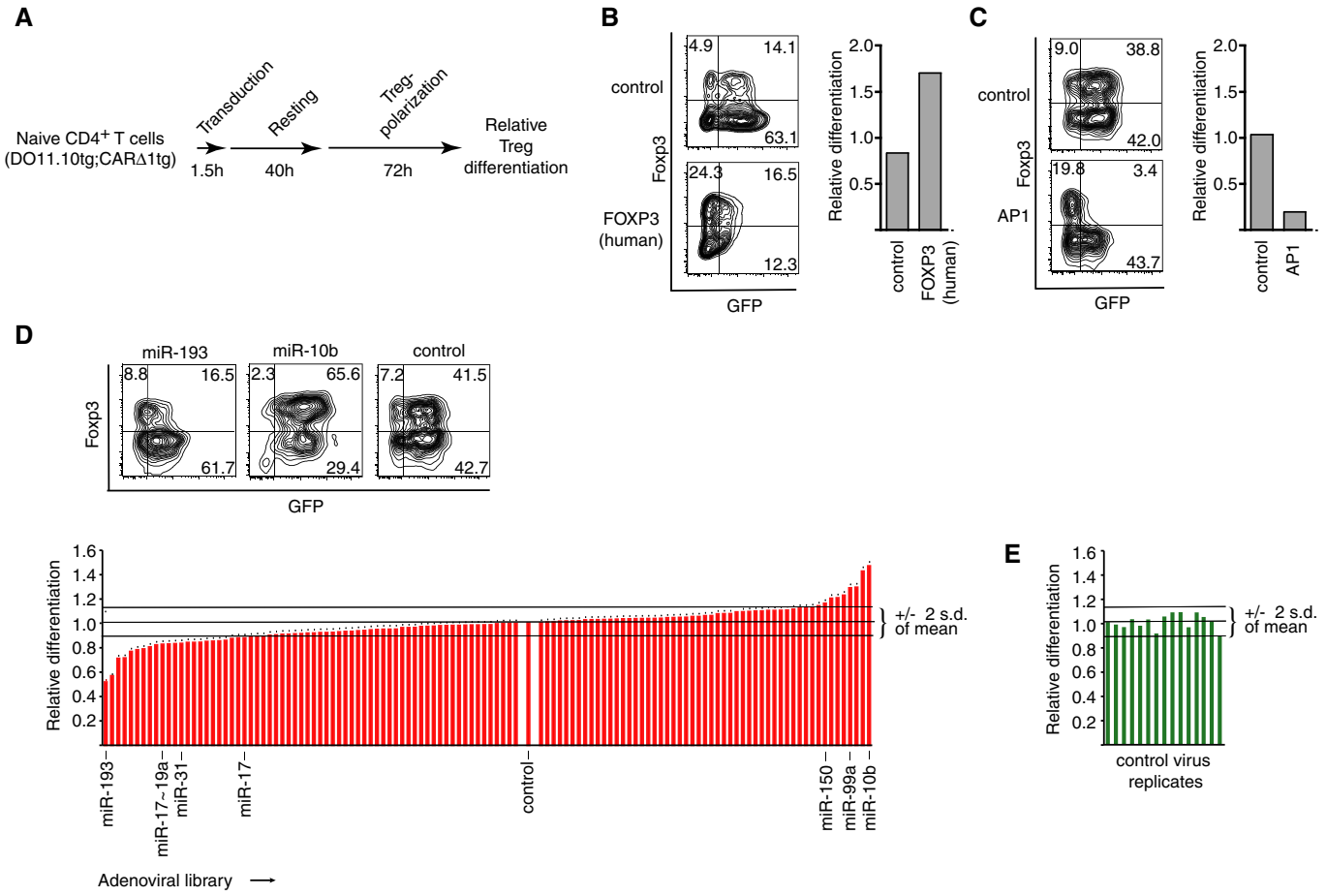

Figure 2. A forward screen to identify miRNAs that regulate Treg cell differentiation.

A Schematic representation of the workflow designed to adenovirally overexpress miRNAs or mRNAs prior to induction of Treg cell differentiation. Naive CD4$^+$ T cells purified from Tg(DO11.10); Tg(CARΔ-1) mice were infected with adenoviruses, rested for 40 h and stimulated under Treg-polarizing conditions.

B, C Treg cell differentiation after ectopic expression of human FOXP3 (B) or AP1 (C). The FACS plots analyze living cells for the expression of the Treg cell marker Foxp3 and the infection marker GFP. The relative differentiation was calculated by dividing the percentage of Foxp3-expressing cells (Foxp3$^+$) among the GFP-expressing cells (GFP$^+$) by the percentage of Foxp3$^+$ cells among the GFP$^-$ cells. The calculated value was termed "relative differentiation" and is shown in the bar diagrams.

D Screening of 130 T-cell-expressed miRNAs during Treg cell differentiation. Exemplary FACS plots show the candidate with strongest positive and strongest negative effect or a control virus with no effect (upper panel). Relative differentiation (bottom panel) was calculated as in (B, C).

E Fifteen control virus replicates were analyzed to calculate mean and SD of the relative differentiation. The miRNAs that caused a shift of the relative differentiation by more than 2 SD above or below mean differentiation of all controls were considered to have a significant effect. Relative differentiation (bottom panel) was calculated as in (B, C).

Data information: The differentiation analyses are representative of four independent experiments (B, C) while the screen was performed once (D, E).

identified miRNAs with a positive effect on Treg cell differentiation (miR-10b, miR-130a, miR-320, miR-99a, miR-146b, miR-296, miR-505, miR-150 and miR-195/497) have no previous history in this particular process. The larger number of effective miRNAs revealed by our screen suggested that not one individual miRNA, but rather a network of interacting miRNAs controls Treg cell differentiation.

We sought to study miRNAs with a marked effect on Treg conversion in our screen during thymic development of regulatory T cells *in vivo* by employing bone marrow reconstitution and lentiviral transductions. We transduced miR-99a as well as miR-140 encoding lentiviral vectors into bone marrow-derived stem cells from mice harboring the human CD2 reporter transgene co-expressed with Foxp3 from IRES sequences (Miyao *et al*, 2012). After reconstitution of lethally irradiated syngenic recipient mice, we found that 6–16% of the thymic CD4-SP T cells expressed the lentiviral marker GFP (Supplementary Fig S2A, right panel). FACS-purified GFP$^+$ thymocytes revealed substantial overexpression of miR-140 or miR-99a in qPCR analyses (Supplementary Fig S2B). However, these cells showed no significant changes in the proportion of Treg cells compared to their GFP$^-$ counterparts (Supplementary Fig S2C). Together, these findings reveal that different from the conversion of naive CD4$^+$ T cells into Tregs, overexpression of miR-140 or miR-99a did not alter thymic Treg cell development. Unfortunately, all mice showed very few GFP-expressing CD4$^+$ T cells in secondary lymphoid organs (Supplementary Fig S2A, left panel), presumably due to reduced promoter activity of the lentivirus in mature T cells, which precluded an analysis of peripheral Treg cell induction *in vivo*.

miRNAs that specifically promote Treg cell differentiation

Pro-inflammatory Th17 cells and anti-inflammatory peripheral Treg cells share a dependency for TGFβ signaling during *in vitro* differentiation. Otherwise, these two programs are reciprocally regulated (Bettelli *et al*, 2006; Veldhoen *et al*, 2006; Yang *et al*, 2008a). Although all miRNAs that affected Treg differentiation are of potential interest for follow-up investigations, we first focused on those miRNAs with reciprocal effects on Th17 cell differentiation. We performed a secondary screen during which adenoviral miRNA overexpression was performed before the samples were divided and stimulated either under Th17-polarizing or under Treg-polarizing conditions. This screen was carried out three times on three successive days and evaluated about half of the potential candidates with a repressive or promoting effect on Treg cell differentiation. Importantly, the results with this confined set of candidates confirmed the initially observed positive or negative effects on Treg cell differentiation (Fig 3A). All miRNAs that we found to repress Treg cell development, except for miR-140, also repressed Th17 differentiation and thus did not impinge on the reciprocal differentiation programs. Interestingly, all analyzed miRNAs with a positive effect on Treg cell development showed either no effect as in the case of miR-130a or reciprocally inhibited Th17 differentiation. We also included miR-100 in the secondary screen, since this miRNA is highly similar to miR-99a from which it differs by only 1 nt outside of an identical seed sequence. miR-99a and miR-100 both showed a reciprocal positive effect on Treg cell and a negative effect on Th17 cell differentiation, although the effect of miR-100 on Treg cell differentiation did not reach significance in the initial screen.

We further investigated how the top candidates miR-10b, miR-100 and miR-99a affected basic cellular processes under Treg cell differentiation conditions. Overexpression of these miRNAs did not affect the viability of T cells (Fig 3B). We also excluded selective effects of miRNAs on the proliferation of T cells. Specifically, we addressed the potential outgrowth of Treg or non-Treg cells within the cultures by discriminating Foxp3$^+$ and Foxp3$^-$ cells (Fig 3C). Double infection of naive CD4$^+$ T cells with a Thy1.1-expressing control virus as well as with a virus that co-expressed the tested miRNA with GFP (Fig 3C, upper panel) showed indistinguishable profiles of proliferation dye dilution when comparing Foxp3$^+$ and Foxp3$^-$ cells (Fig 3C, middle and lower panels). Furthermore, these profiles were also very similar in the respective control cells that received two control viruses that expressed either Thy1.1 or GFP (Fig 3C, middle and lower panels). To assess whether overexpression of miR-10b, miR-100 or miR-99a in naive CD4$^+$ T cells altered their activation status or potential, we overexpressed the miRNAs and stained for different markers that are able to discriminate naive and activated T cells. We analyzed CD4$^+$ T cells prior to or after activation under Treg-polarizing conditions. The expression levels of the markers on GFP-expressing cells were very similar in the miRNA-transduced compared to control-transduced cells and documented the naive state (CD62L$^+$ and CD44$^-$) prior to activation (Fig 3D, 40 h rest). Within each sample, the cells uniformly lost the expression of CD62L and upregulated the expression of CD44 upon activation with anti-CD3/anti-CD28-coupled beads (Fig 3D, 40 h rest + 18 h activation). Additional experiments with combined anti-CD5/anti-IL7R and anti-CD25/anti-CD69 stainings confirmed these results and also argued against a general effect on T-cell quiescence, T-cell receptor signal strength or T-cell activation due to overexpression of the individual miRNAs (Supplementary Fig S3A and B). Altogether, these data show that overexpression of miR-99a, miR-100 or miR-10b in naive T cells neither alters the naive state nor the capacity or sensitivity of the T cells to become activated under Treg-polarizing conditions.

miR-99a as well as miR-150 can repress *Mtor*

The reciprocal function of the candidate miRNAs during Treg/Th17 cell differentiation prompted us to ask whether these miRNAs repressed an mRNA with a crucial role in the development of these two CD4$^+$ T-cell subsets. We focused on studying target mRNAs of miR-99 and miR-100. Using the online tool TargetScanMouse 6.2 (http://www.targetscan.org/), a search for miR-99a targets identified 46 genes, including *Mtor*. mTOR, as part of the mTORC1 complex, is a driver of Th17 differentiation. Deletion of the *Mtor* gene in CD4$^+$ T cells abrogates effector T-cell differentiation and instead promotes Treg cell development (Delgoffe *et al*, 2009; Shi *et al*, 2011). Within the *Mtor* 3′ UTR, a total of four different conserved miRNA target sites are predicted with one of these being a site of miR-99a/miR-99b/miR-100 recognition. To validate

Figure 3. miR-99a, miR-100 and miR-10b selectively promote Treg cell differentiation.

A Overexpression of miR-99a, miR-100 and miR-10b promotes Treg but not Th17 cell differentiation. Results of a secondary screen with naive CD4$^+$ T cells transduced to express selected candidate miRNAs followed by stimulation under Treg- or Th17-polarizing conditions (compare Fig 2A). The bar diagram shows means ± SD of three independent experiments. Asterisks represent *P*-values of the comparison of either sample with the control calculated by Student's *t*-test without multiple sample correction.

B Overexpression of miR-99a, miR-100 and miR-10b has no influence on T-cell viability. Naive CD4$^+$ T cells were transduced to express the indicated miRNAs and then differentiated into regulatory T cells (compare Fig 2A). Cell viability was analyzed using a dye staining dead cells. FACS plots are representative of four independent experiments.

C The proliferation of Foxp3$^+$ and Foxp3$^-$ T cells is not influenced by the overexpression of miR-99a, miR-100 or miR-10b. Naive CD4$^+$ T cells were labeled with a proliferation dye and infected with a control adenovirus expressing the Thy1.1 marker together with a second adenovirus expressing the indicated miRNA-IRES-GFP or GFP control viruses. Cells were mixed and rested for 40 h and subsequently stimulated under Treg-polarizing conditions. After 72 h, the expression of Foxp3 and infection markers as well as the dilution of the proliferation dye was analyzed by flow cytometry. Top panel: FACS analyses of Thy1.1 and GFP expression. Lower panels: Histogram presents the overlay of Foxp3$^-$ cells (red areas) and Foxp3$^+$ cells (blue lines) in the Thy1.1$^+$/GFP$^-$ gate (upper panel) or in the Thy1.1$^-$/GFP$^+$ gate (lower panel). Data are representative of three independent experiments.

D Quiescence and activation are unchanged in T cells expressing miR-99a, miR-100 or miR-10b. Naive CD4$^+$ T cells were transduced to express the indicated miRNAs (compare Fig 2A). Cells were either rested for 40 h (upper panel) or rested for 40 h combined with subsequent stimulation for 18 h under Treg-polarizing conditions (lower panel). Expression of the activation markers CD62L and CD44 was analyzed by flow cytometry in infected cells (GFP$^+$). The data are representative of four independent experiments.

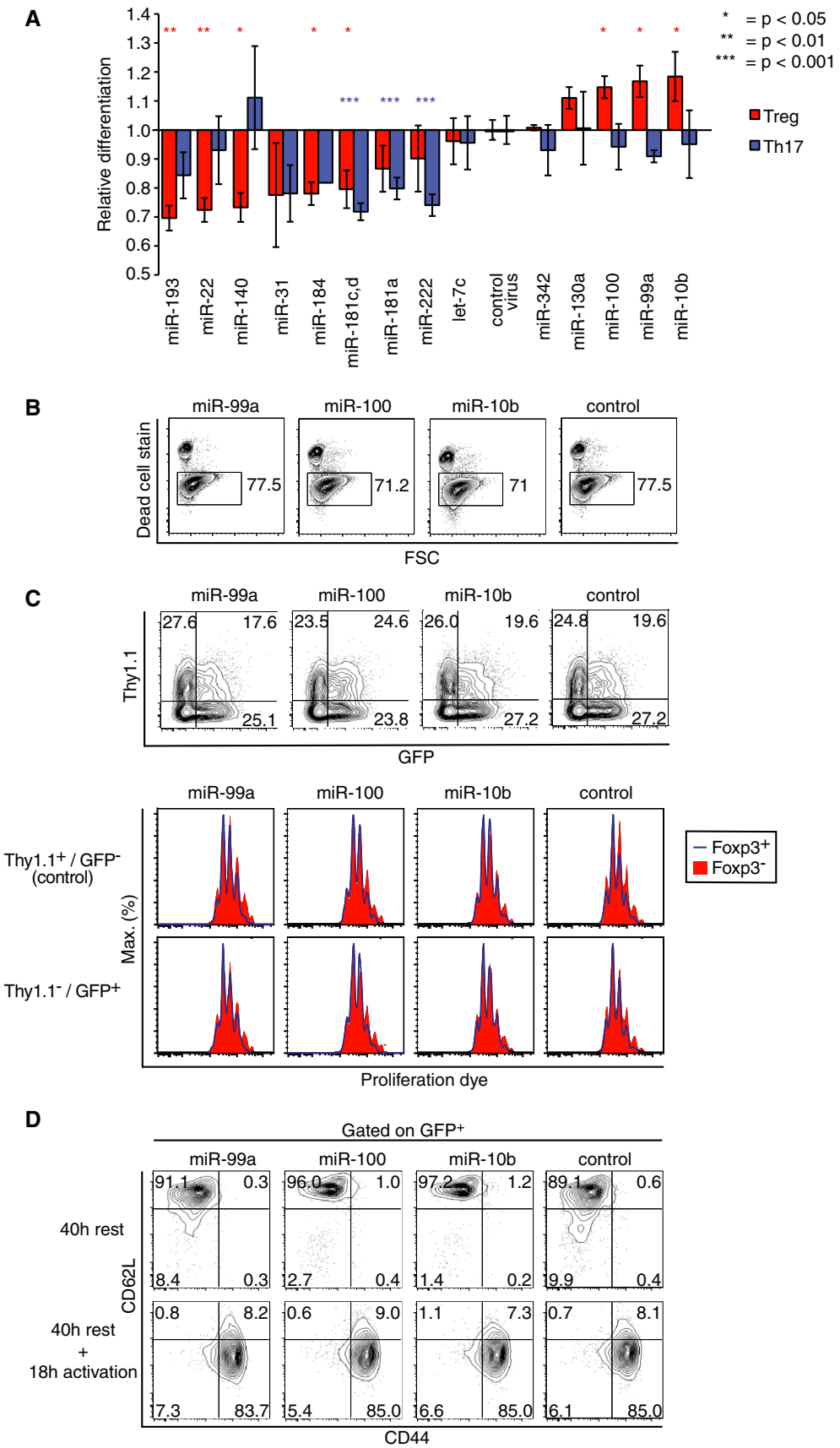

Figure 3.

this *in silico* result in luciferase assays, the 827 nt long 3′ UTR of *Mtor*, either in its wild-type form or with a mutated miR-99/miR-100 binding site (Fig 4A), was cloned downstream of a *Renilla* luciferase gene into a dual luciferase reporter vector. The resulting adenoviral reporter constructs were then co-transduced with miR-99a-encoding or control viruses into wild-type mouse embryonic fibroblast (MEF) cells. Indeed, miR-99a was able to significantly inhibit the *Renilla* luciferase activity (Fig 4B, left panel). In line with previous data (Oneyama *et al*, 2011), this repression depended on the predicted miR-99 binding site in the *Mtor* 3′ UTR, because mutating three nucleotides in the respective target sequence (Fig 4A) completely reversed the repression by miR-99a (Fig 4B, right panel). To demonstrate that the observed miR-99a-mediated repression of *Mtor* occurs in T cells, we adenovirally transduced naive $CD4^+$ T cells with miR-99a or controls that included empty vector and miR-10b. We confirmed the expression and correct processing of both miRNAs using qPCR assays that were designed to specifically detect the respective mature forms (Fig 4C, left panel). After 18 h of T-cell activation, protein lysates were prepared and the different cell samples were analyzed in immunoblots to detect mTOR. The result demonstrated downregulation of the mTOR protein level as a consequence of miR-99a expression. Consistently, with miR-10b having no predicted target site in the *Mtor* 3′ UTR, there was no effect on mTOR protein after miR-10b overexpression in primary T cells (Fig 4C, right panel).

We inspected the 3′ UTRs of *Mtor* for other regulatory elements and noticed an additionally predicted miR-150 binding site (Fig 4D). Interestingly, in our Treg cell differentiation screen (Fig 2D), miR-150 was among the identified ten miRNAs with a positive effect on Treg cell differentiation. As for miR-99a, we could confirm the biological function of the miR-150 target sites in the *Mtor* 3′ UTR using luciferase assay experiments (Fig 4E, left panel). Results obtained from mutating the miR-150 target site in the *Mtor* 3′ UTR provided unambiguous proof that *Mtor* is a direct target of miR-150 repression (Fig 4E, right panel). In sum, both miR-99a and miR-150 bear the potential to repress mTOR, a critical driver of Th17 cell differentiation.

Expression of miR-99a is strongly induced by retinoic acid

In order to characterize the relative importance of miR-99a and miR-150 during Treg cell induction, we determined their expression profiles during the first 72 h of stimulation (Fig 5A). The expression levels of the mature miR-99a and miR-150 decreased after 36 h. We further found that the overall expression levels of miR-150 were very high, while those of miR-99a were much lower (Fig 5B). These data raised the question whether miR-99a may be effective even at low expression levels or whether it particularly contributes to Treg cell differentiation under conditions that induce its expression. Since TGFβ promotes Treg cell differentiation, we first tested miRNA expression under different TGFβ concentrations. However, activating naive $CD4^+$ T cells with or without increasing concentrations of TGFβ for 18 h had no influence on the expression levels of the miRNAs (Fig 5C). All-*trans* retinoic acid (ATRA) has been implicated, for example, in the regulation of miR-10b in neuroblastoma cells (Foley *et al*, 2011; Meseguer *et al*, 2011). In our Treg cell differentiation experiment, ATRA treatment had only a minor effect on miR-150 expression, but it resulted in a pronounced sixfold upregulation of miR-99a levels (Fig 5C, right and left panel). Since it is known that retinoic acid increases TGFβ-induced expression of Foxp3 (Mucida *et al*, 2007; Nolting *et al*, 2009), the uncovered regulation along the ATRA-miR-99a-mTOR axis provides an important detail in the network that controls Treg/Th17 cell differentiation.

Endogenous miR-150 levels are required for the induction of Treg cells

In order to study the importance of the highly expressed miR-150 in Treg cell differentiation, we made use of a neutralizing antagomir (Krützfeldt *et al*, 2005; Stittrich *et al*, 2010). Treating naive $CD4^+$ T cells prior to activation with an antagomir directed against miR-150 substantially reduced the expression level of mature miR-150 when compared to a scramble control (Fig 6A). When tested for their effect on Treg cell induction, we observed diminished frequencies of $Foxp3^+$ cells in the antagomir-150-treated compared to the untreated or scrambled antagomir samples (Fig 6B). Notably, concentrations of the scramble antagomir higher than 2 μM resulted in cell death and increased Treg cell differentiation (Fig 6B). Nevertheless, antagomir-150-treated compared to scramble antagomir-treated samples consistently displayed a reduction in Treg cell differentiation over the increasing oligo concentrations (Fig 6C). We next analyzed spontaneous Treg cell differentiation of antagomir-treated T cells from congenic Foxp3 (GFP) reporter mice after transfer into Rag2-deficient recipients. Fourteen days after adoptive transfer of FACS-purified naive $CD4^+$ T cells that were negative for CD25 and Foxp3(GFP), we found a significant reduction of spontaneous Treg conversion in cells that were treated with the antagomir against miR-150 compared to scramble control (Fig 6D). These data confirmed our *in vitro* differentiation data and demonstrated the importance of physiological levels of miR-150 expression.

An intact miR-99a target site is a prerequisite for miR-150-mediated regulation of *Mtor*

Using luciferase assays in wild-type cells with endogenous miRNAs, we demonstrated that miR-99a and miR-150 can repress *Mtor;* however, the relative contribution of each of the miRNAs to the regulation was unclear. To address this issue, we performed luciferase assays in the $Dicer^{-/-}$ MEF cell clone 2G4 that we recently generated and which is devoid of almost all endogenous miRNAs (Glasmacher *et al*, 2010; Parameswaran *et al*, 2010). Despite *Dicer* deficiency, overexpression of miR-99a and miR-150 was possible when we "reprogrammed" the backbone of the Dicer-independent pre-miR-451 (Cifuentes *et al*, 2010; Yang *et al*, 2010), as indicated in Fig 7A. In this context, the slicer activity of Ago2 replaces Dicer function and produces mature miR-99a-5p and miR-150-5p from the respective pre-miR-451 constructs. According to the Dicer-independent biogenesis of these mature miRNAs, we termed them "miR-99a (Dicer-ind.)" and "miR-150 (Dicer-ind.)" (Fig 7A). To test our system, reprogrammed miRNAs were adenovirally transduced into $Ago2^{-/-}$, $Dicer^{-/-}$ or wild-type MEF cells, and the expression of processed, mature miR-99a and miR-150 was quantified using qPCR assays. As expected, the miR-451 backbone-derived miRNAs were significantly overexpressed independently of Dicer; however, the processing clearly required Ago2 (Fig 7B). In wild-type MEF

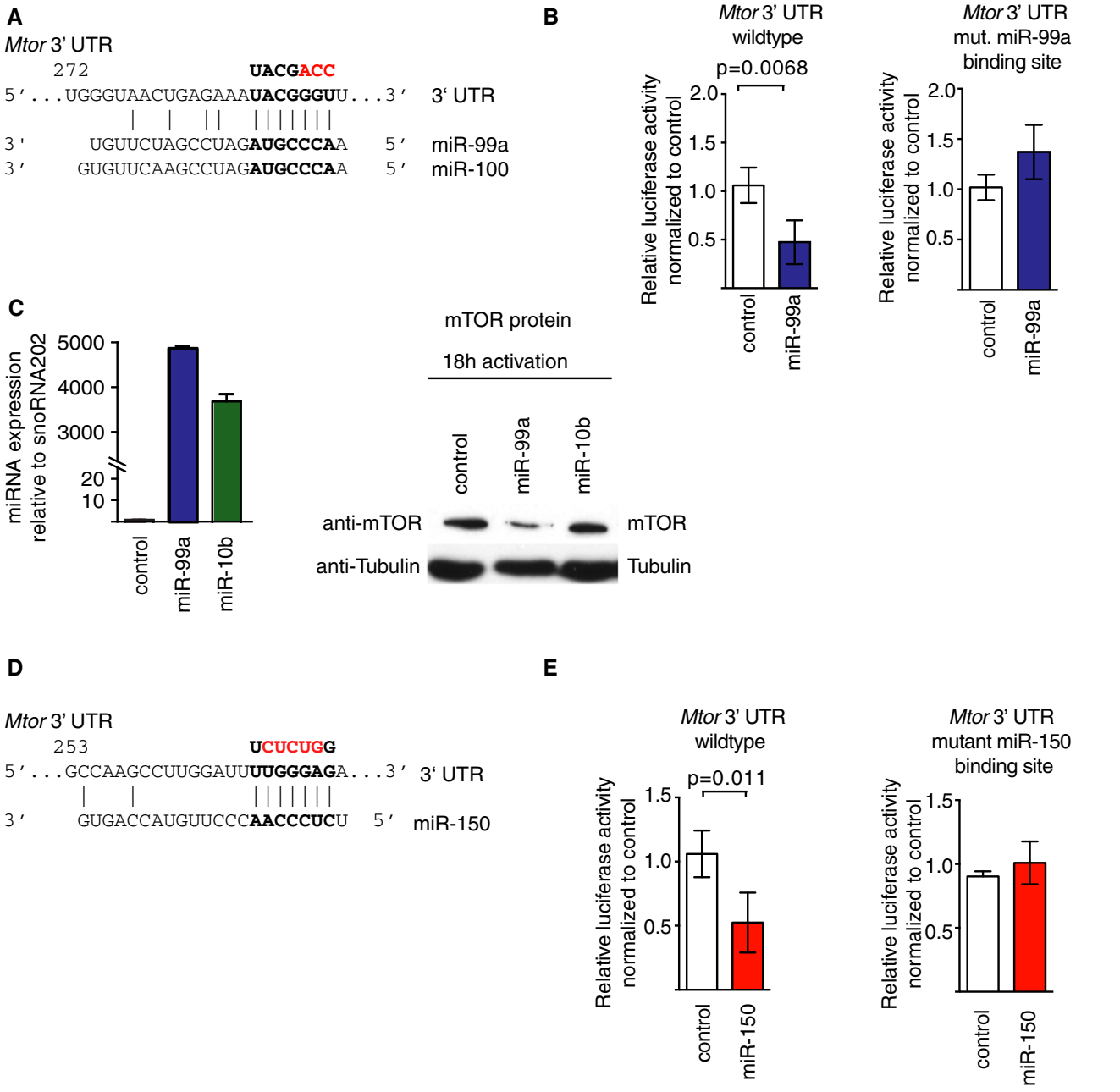

Figure 4. miR-150 as well as miR-99a directly repress the *Mtor* 3′ UTR.

A Predicted base-pairing of miR-99a and of miR-100 with the target sequence in the 3′ UTR of *Mtor*. The seed sequence in the miRNA and the complementary sequence in the 3′ UTR are displayed in bold letters. Mutations introduced in the target sequence are shown in red. The numbers indicate the position within the *Mtor* 3′ UTR.

B miR-99a repression is dependent on the predicted target site in the *Mtor* 3′ UTR. MEF cells were infected with adenoviruses encoding the *Mtor* 3′ UTR dual luciferase reporter construct in its wild-type version (left panel) or in a miR-99a target site-mutated version (right panel). The cells were co-infected with miR-99a-encoding or control viruses. After 48 h, the cells were lysed and relative luciferase activities were determined. The bars represent means ± SD of four independent experiments, and statistical significance was calculated using Student's *t*-test.

C miR-99a overexpression reduces mTOR protein levels in primary T cells. $CD4^+$ T cells were transduced to express the indicated miRNAs and activated under Treg-polarizing conditions for 18 h. miRNA overexpression was determined by qPCR showing the average of two technical replicates, and the results of control virus-infected samples were set to 1 (left panel). Protein expression of mTOR was determined by Western blot analysis (right panel). Data are representative of two independent experiments.

D Predicted base-pairing of miR-150 with the target sequence in the 3′ UTR of *Mtor*. The seed sequence in the miRNA and the complementary sequence in the 3′ UTR are displayed in bold letters. Mutations introduced in the target sequence are shown in red. The numbers indicate the position within the *Mtor* 3′ UTR.

E miR-150 directly represses *Mtor*. MEF cells were infected with adenoviruses encoding the *Mtor* 3′ UTR dual luciferase reporter construct in its wild-type version (left panel) or in a miR-150 target site-mutated version (right panel). The cells were co-infected with miR-150-encoding or control viruses. After 48 h, the cells were lysed and relative luciferase activities were determined. The bars represent means ± SD of four independent experiments, and statistical significance was calculated using Student's *t*-test.

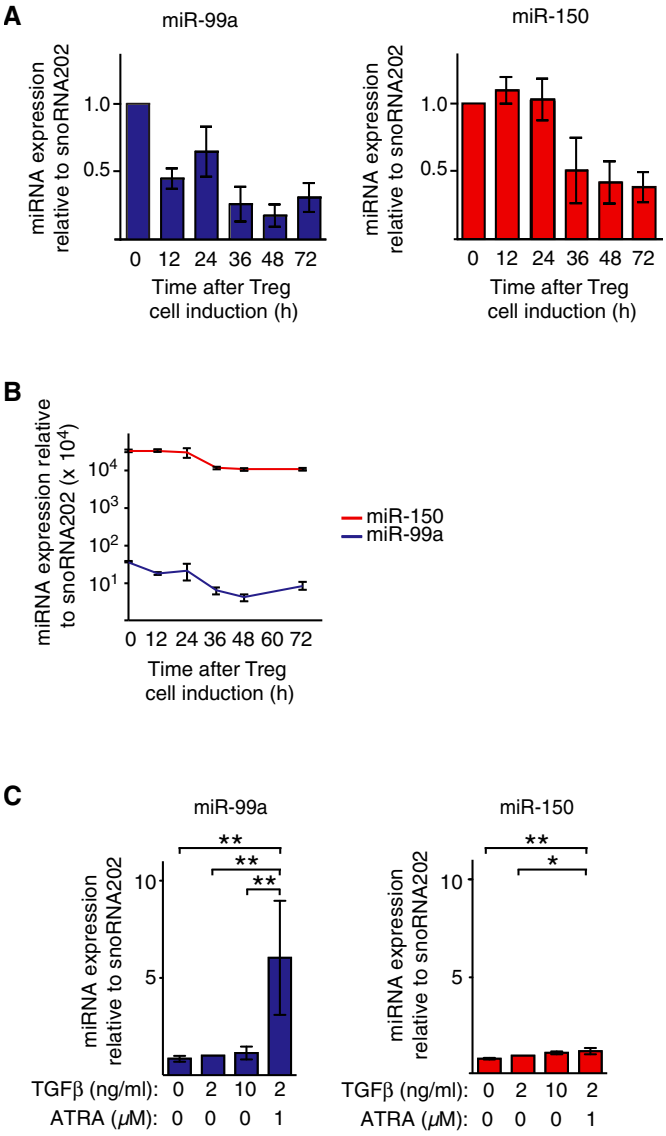

Figure 5. All-*trans* retinoic acid induces miR-99a expression during Treg induction.

A Relative miRNA expression levels during Treg cell differentiation. Naive $CD4^+$ T cells were stimulation under Treg cell-polarizing conditions for 72 h to monitor endogenous miR-99a and miR-150 expression by quantitative qPCR at the indicated time points. miRNA expression levels at the 0 h time point were set to 1. Data are representative of three independent experiments. Error bars indicate technical variance of qPCR.

B Same experiment as shown in (A) monitoring the endogenous expression levels of miR-99a and miR-150 without normalization.

C All-*trans* retinoic acid strongly induces miR-99a expression. Naive $CD4^+$ T cells were stimulated for 18 h either under standard Treg-polarizing conditions (2 ng/ml TGFβ), or with medium and varying TGFβ concentrations or with medium supplemented with 2 ng/ml TGFβ and 1 μM ATRA. miRNA expression was measured using qPCR assays and normalized to the results of standard conditions (2 ng/ml TGFβ). Data represent means ± SD of two (0 and 10 ng/ml TGFβ) or of five (2 ng/ml TGFβ, 2 ng/ml TGFβ + 1 μM ATRA) independent experiments. Statistical significance was calculated by ANOVA followed by Tukey's multiple comparison tests, $*P < 0.05$, $**P < 0.01$. Please note that due to the high degree of sequence similarity, we cannot exclude that the miR-99a qPCR assay can also detect miR-100.

cells, overexpression of both *Dicer*-independent miRNAs miR-99a and miR-150 equally repressed the *Mtor* 3′ UTR reporter activity to ~60% (Fig 8A). In *Dicer*-deficient MEF, expression of miR-99a (Dicer-ind.) repressed the reporter activity almost to the same extent as in wild-type MEF. Surprisingly, the repressive effect of miR-150 (Dicer-ind.) in wild-type cells was abolished in cells that lacked Dicer (Fig 8A). These data suggested a strong regulation of the *Mtor* 3′ UTR by miR-99a independent of other miRNAs, while miR-150-mediated regulation depended on the cooperation with other miRNAs, possibly miR-99a.

The sequences in the mouse *Mtor* 3′ UTR that are complementary to the seed sequences of miR-99a and miR-150 are separated by only 24 nucleotides, providing a context for cooperative function. Binding of the miRNA-loaded RISC complex to one site may influence the function of the other. To further test cooperation on the level of the binding sites, we mutated the target sites for miR-99a or miR-150 in the *Mtor* 3′ UTR or left them unaltered and transduced the resulting constructs into wild-type or *Dicer*-deficient MEF cells. The cells were co-infected with a 1:1 mixture of viruses to co-express miR-99a (Dicer-ind.) and miR-150 (Dicer-ind.). With functional binding sites present, the combined expression of miR-99a and miR-150 effectively reduced luciferase activity in wild-type as well as in *Dicer*-deficient cells.

When we expressed the *Mtor* 3′ UTR reporter with a mutated miR-150 target site together with Dicer-independent miR-99a and miR-150, the luciferase activity showed miRNA-dependent repression in wild-type cells. Despite having an intact miR-99a binding site, the repression of this reporter construct was already diminished compared to the repression observed for the wild-type 3′ UTR. Similarly, the *Mtor* 3′ UTR with the miR-150 target sequence mutation expressed in *Dicer*-deficient cells revealed an even smaller and non-significant repression after combined miRNA overexpression (compare Fig 8B and C). This suggests that the mutation in the miR-150 binding site negatively affected the context of miRNA-mediated regulation even at a distinct miR-99a site. Nevertheless, the mutation of the miR-99a target site in the *Mtor* 3′ UTR completely abrogated reporter repression, regardless of the functional miR-150 binding site and overexpression of miR-150 (Fig 8B). This mutant was similarly insensitive to miRNA-mediated repression in the presence or absence of endogenous miRNAs (Fig 8B and C). Together, these results promote a concept of cooperative miRNA repression. We propose that strong cooperative repression of *Mtor* is achieved when both miRNAs are present. Mechanistically miR-99a-mediated *Mtor* repression did not require target mRNA binding by other miRNAs, while miR-150 was only active when miR-99a was bound to its adjacent target site in the *Mtor* 3′ UTR.

Discussion

In this study, we have defined an experimental window within the first 12–36 h of T-cell stimulation during which miRNAs can potently influence the differentiation of naive $CD4^+$ T cells into Treg cells. Adenoviral gene transfer into naive $CD4^+$ T cells enabled us to overexpress miRNAs during this time. A parallel screen of 130 miRNAs on 108 adenoviral constructs identified 21 constructs containing 29 miRNAs that inhibited and nine constructs containing 10 miRNAs that promoted the generation of Treg cells (Fig 2). These

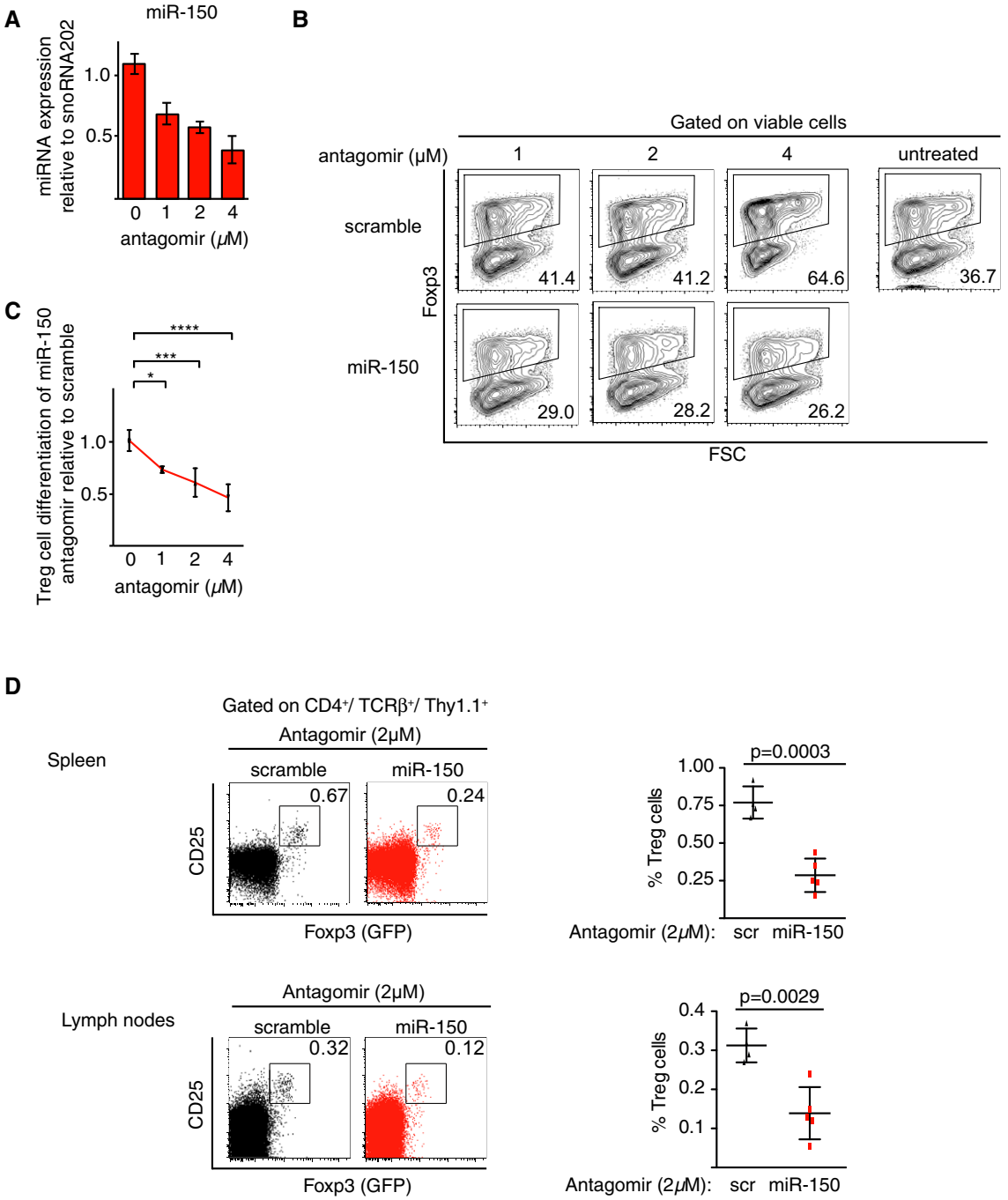

Figure 6. Importance of miR-150 expression during Treg cell induction.

A An antagomir against miR-150 reduces mature miR-150 expression in T cells. Naive $CD4^+$ T cells were incubated with an antagomir complementary to mouse miR-150 or a scramble control and rested for 24 h. Cells were then stimulated under Treg-polarizing conditions. After 18 h, the expression of mature miR-150 was determined by qPCR relative to endogenous expression levels. Data show the average and variance of two technical replicates and are representative of four independent experiments and are displayed with the scramble antagomir treatment set to 1.

B, C Reduction of miR-150 expression interferes with Treg cell differentiation. Naive $CD4^+$ T cells were incubated with an antagomir complementary to mouse miR-150 or a scramble control, rested for 24 h and then stimulated under Treg-polarizing conditions for 72 h. Foxp3 expression was analyzed by flow cytometry. Data are representative FACS plots (B) or show means ± SD of four independent experiments, and statistical significance was calculated by ANOVA followed by Tukey's multiple comparison tests (C), $*P < 0.05$, $***P < 0.001$, $****P < 0.0001$.

D miR-150 knockdown interferes with Treg cell differentiation *in vivo*. Naive $CD4^+$ T cells were FACS-sorted from BALB/c.Thy1.1 × Dereg × DO11.10 mice. Prior to adoptive transfer into BALB/c.$Rag2^{-/-}$ mice, the cells were incubated for 2 h with an antagomir complementary to mouse miR-150 or a scramble control. Representative flow cytometry of Foxp3 (GFP) and CD25 expression among transferred $CD4^+$ T cells from spleen or lymph nodes (left panels) at day 14 after adoptive transfer. Percentages of $Foxp3^+$ cells among transferred cells from two independent experiments that are depicted in the diagrams are shown as means ± SD. Each symbol represents an individual mouse (n = 5–6). Statistical significance was calculated using Student's t-test.

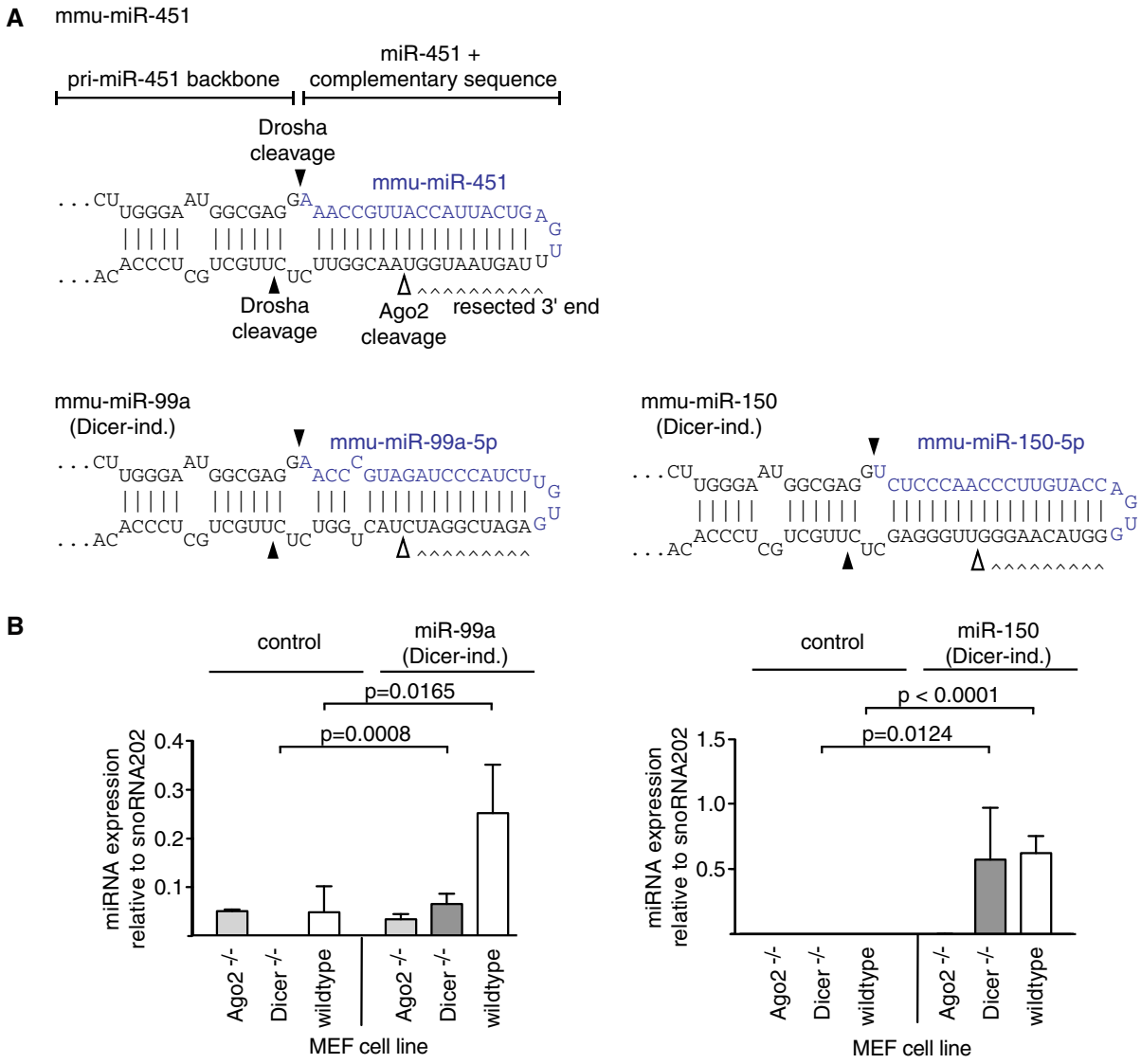

Figure 7. Dicer-independent expression of miR-99a and miR-150.

A Schematic depiction of pri-miR-451 and the reprogrammed miR-451 variants. The mature miRNA sequences are shown in blue.

B Dicer-independent miRNAs are expressed in *Dicer*$^{-/-}$ *cells*. Wild-type MEF, *Ago2*$^{-/-}$ MEF or *Dicer*$^{-/-}$ MEF cells were infected with adenoviruses encoding miR-99a (Dicer-ind.), miR-150 (Dicer-ind.) or control viruses. Expression of the indicated mature miRNA was quantified by qPCR. Data represent means ± SD of three independent experiments, and *P*-values were calculated using Student's *t*-test.

results promote a concept in which not one single miRNA, but rather a network of miRNAs with shared and individual mRNA targets supports the establishment of Treg cell identity. Consistently, we demonstrate *Mtor* as a common target of two Treg-promoting miRNAs, miR-99a and miR-150 and analyzed the regulatory interplay of miR-99a and miR-150 with their respective target sites in the *Mtor* 3′ UTR. We specifically studied the regulation in a system that is largely devoid of endogenous miRNAs. Although much more can be learned about these interactions, our data implicate a so far unknown mechanism by which the absence of one miRNA neutralizes the activity of another.

Comparing the effects of miRNAs in our screen with the published function of the respective miRNAs in T helper cell differentiation showed a large degree of overlap. Of note, there are differences that are likely to be explained either by the different experimental approaches that involved loss- or gain-of-function or by the differences in the timing and/or level of overexpression.

In our analysis, miR-10b strongly promoted Treg cell differentiation. Surprisingly, its paralog miR-10a had no effect in our screen. This is consistent with previously published results, showing that miR-10a deletion had no influence on the differentiation of Treg cells (Jeker *et al*, 2012). Instead, miR-10a appeared to be involved in Treg cell plasticity as it prevented conversion of TGFβ-induced Treg cells into follicular helper T cells and negatively influenced Th17 cell differentiation when overexpressed retrovirally (Takahashi *et al*, 2012). Similarly, miR-146a, which is important in mature Treg cells

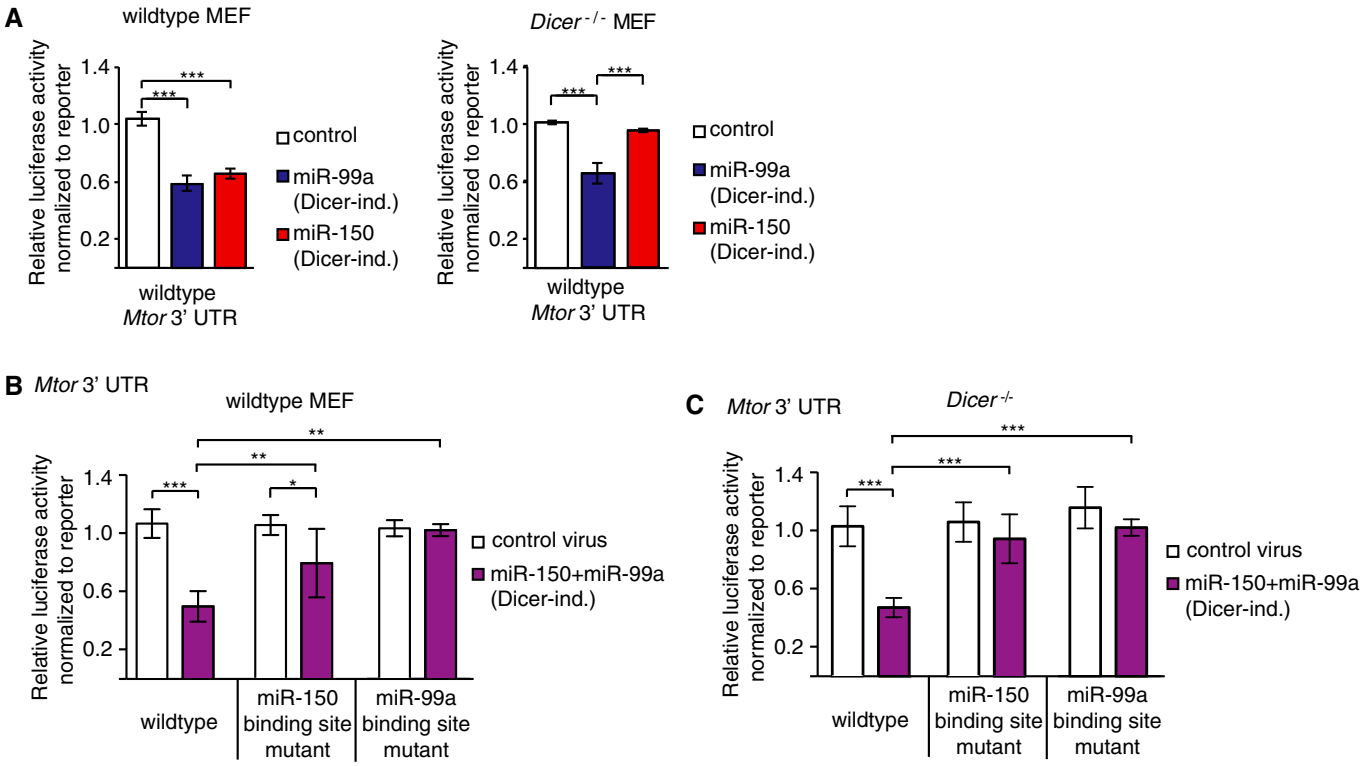

Figure 8. Cooperative repression of the *Mtor* 3′ UTR by miR-150 and miR-99a.

A miR-99a but not miR-150 represses *Mtor* in the absence of other miRNAs. Wild-type MEF or *Dicer*$^{-/-}$ MEF cells were adenovirally infected to express a wild-type *Mtor* 3′ UTR dual luciferase reporter construct. Cells were co-infected with adenoviruses encoding Dicer-independent miR-99a, miR-150 or control viruses at an MOI of 100. After 48 h, the cells were lysed and relative luciferase activities were determined. The values represent means ± SD from three independent experiments, and statistical significance was calculated using ANOVA followed by Tukey's multiple comparison test, ***$P < 0.001$.

B, C An intact miR-99a binding site is required for cooperative *Mtor* regulation by miR-99a and miR-150. Wild-type MEF (C) or *Dicer*$^{-/-}$ MEF cells (D) were infected with adenoviruses encoding *Mtor* 3′ UTR dual luciferase reporter constructs in its wild-type or miR-150- or miR-99a-mutated binding site versions. Cells were co-infected with a control adenovirus or with a mix of adenoviruses encoding miR-99a (Dicer-ind.) and miR-150 (Dicer-ind.) each at an MOI of 50. After 48 h, the cells were lysed and relative luciferase activities were determined. The values represent means ± SD from four (B) or six (C) independent experiments, and statistical significance was calculated using ANOVA followed by Tukey's multiple comparison test, *$P < 0.05$, **$P < 0.01$, ***$P < 0.001$.

(Lu *et al*, 2009, 2010), showed inhibitory effects on Treg cell differentiation in our screen. In contrast, we found that miR-146b, whose 5p miRNA sequence differs from the miR-146a sequence by only two nucleotides, promoted Treg cell differentiation. Obviously, paralogous miRNAs can exert opposing effects due to differential target selection. Another possible way to bring together the divergent results is that the individual experimental approaches could selectively show effects related to 5p or 3p miRNAs, which have been shown to be able to exert opposing functions (Zhou *et al*, 2010).

In our screen, miR-155 overexpression exhibited a negative effect on Treg cell differentiation suggesting a potential role of miR-155 in reciprocal Th17/Treg lineage decisions. Consistently, O'Connell *et al* have demonstrated that miR-155 positively influences Th17 cell differentiation (O'Connell *et al*, 2010). In addition, Du *et al* (2009) reported a promoting effect selectively on Th17 differentiation for miR-326 and no effect on Treg cell differentiation, which was also the case in our screen. Finally, the here identified negative effects of all constructs containing individual or clustered miR-17~92 miRNAs on Treg cell differentiation are in line with a previous report (Jiang *et al*, 2011). In fact, reconstitution of miR-17~92 cluster deficient T cells with miR-17 or miR-19b alone blocked Treg cell differentiation and promoted Th1 cell differentiation (Jiang *et al*, 2011). Noteworthy, the previously published study applied retroviral transduction that overexpresses the miRNAs late in Treg cell differentiation. This suggests that the miR-17~92 cluster can influence Treg cell differentiation at early and late stages. Although having a negative impact on differentiation, the miR-17~92 cluster was also required for proper function of Tregs and their ability to produce L-10 (De Kouchkovsky *et al*, 2013). Such differential functionality may even be reinforced by strong changes in the abundance of the miRNA loaded onto the miRISCs before and after downregulation of Ago proteins that occurs at the time when Treg cell identity is being established (Fig 1 and Bronevetsky *et al*, 2013).

Our screen has identified new miRNAs with a repressive function and, more importantly, the first ten miRNAs that promote the development of regulatory T cells, namely miR-10b, miR-130a, miR-320, miR-99a, miR-146b, miR-296, miR-505, miR-150 and miR-195/497. We investigated the effects of some of these miRNAs in more detail. For miR-10b, miR-99a and the highly similar miR-100, we could demonstrate that their promoting effect is specific for the differentiation program of induced Treg cells, as we determined a negative influence on Th17 differentiation.

miR-99a and miR-100 belong to the same miRNA family and both promoted Treg cell differentiation in our experiments. miR-99b showed no effect, potentially because this third family member differs from miR-99a by one nucleotide inside and by two nucleotides outside of the seed sequence. Moreover, different from the other family members, miR-99b was overexpressed from a clustered construct that also included miR-125 and let-7e, which could affect the miR-99b expression level or neutralize its specific effect. Our experiments showed that miR-99a targets *Mtor* in T cells and promotes Treg cell differentiation. miR-99a and miR-100 have been shown to be downregulated in various cancer cells, and there is already evidence for mTOR, which promotes cell growth and is required for proliferation, to be a target of both miRNAs (Nagaraja *et al*, 2010; Oneyama *et al*, 2011). miR-99a was found upregulated in response to irradiation of a radiosensitive cancer cell line (Mueller *et al*, 2012). In this study, it was shown that miR-99a targets the chromatin-remodeling factor SNF2H, which interfered with DNA repair as part of the SWI/SNF complex. This complex can differentially regulate chromatin accessibility in T cells and induced the expression of AP1 (Mueller *et al*, 2012). Since AP1 activity strongly interfered with Treg cell induction (Fig 2C), its putative downregulation by miR-99a or miR-100 may be another node in the miRNA: target mRNA network that operates in Treg cell differentiation.

The reciprocal regulation of T-cell differentiation by miR-99a led us to search for a target mRNA encoding a factor that interferes with Treg and promotes Th17 cell differentiation. Our data demonstrate *Mtor* mRNA as a direct target of miR-99a in T cells. We did not observe an effect of miR-99a overexpression during thymic Treg development. This is likely due to the different molecular requirements for thymic and peripheral Treg cell induction that also become obvious from genetic ablation of the miR-99a target *Mtor*, which had no effect on thymic Treg development but strongly biased T-cell differentiation toward a Treg instead of a Th17 phenotype (Delgoffe *et al*, 2009). Endogenous miR-150 levels were essential for Treg cell differentiation *in vitro* and *in vivo*, and overexpression of this miRNA not only promoted Treg cell differentiation in our screen, but also repressed *Mtor* through a binding site that is only 24 nt upstream of the miR-99a target site. This suggested cooperative target regulation. Studies on cooperative effects of miRNAs have so far been conducted in the context of endogenous miRNA expression (Grimson *et al*, 2007; Sætrom *et al*, 2007; Broderick *et al*, 2011). These studies established general requirements for cooperativity of miRNA-binding sites in terms of spacing and extent of sequence complementarity. They also demonstrated that all four Argonaute proteins can regulate targets in a cooperative manner (Broderick *et al*, 2011). Comparing cells that are largely devoid of endogenous miRNAs with wild-type cells, we show that endogenous miRNAs can confound the study of cooperative repression (Fig 8). Reprogrammed miR-451 constructs have emerged as a straightforward approach to express a miRNA in an Ago2-dependent manner (Cifuentes *et al*, 2010; Yang *et al*, 2010, 2012; Dueck *et al*, 2012; Yoda *et al*, 2013) and allowed us to analyze cooperation of miR-99a and miR-150 in *Dicer*-deficient cells. Different from Drosha/Dicer-dependent miRNAs, these constructs selectively express either the 5p- or the 3p-encoded miRNA irrespective of the surrounding context (Fig 7). While miR-99a alone could repress the *Mtor* 3′ UTR reporter in *Dicer*-deficient cells, miR-150 depended on miR-99a. These results indicated that the *Mtor* 3′ UTR not only encodes miRNA-binding sites that enable cooperation, but that cooperation is actually obligatory for miR-150-mediated *Mtor* repression. Consistently, mutation of the miR-99a binding site largely abrogated *Mtor* reporter repression by combined miR-99a and miR-150 expression, supporting the essential role of miR-99a. The observed cooperativity is likely to be caused through the vicinity of the two *cis*-elements in the 3′ UTR that are recognized by miR-99a and miR-150. Recent evidence reveals distinct sequence-encoded secondary structures in mRNAs with a general importance for gene regulation (Wan *et al*, 2014). It highlights the importance miRNA-binding site accessibility (Wan *et al*, 2014), which may determine the sequential recruitment of miRNA-loaded RISC complexes as well as their interaction with cofactors. We propose that cooperativity on the one hand increases the impact of the individual miRNA and on the other hand can create functional dependency of several miRNAs in a specific biological context. Relating our mechanistic findings to expression levels, we propose that miR-150, which is constantly present at high levels during differentiation of naive $CD4^+$ into regulatory T cells, efficiently represses *Mtor* in cooperation with other miRNAs. Upon exposure of T cells to retinoic acid, the lowly expressed miR-99a becomes upregulated, which then enables efficient *Mtor* repression in cooperation with miR-150 to enhance Treg cell differentiation. Taken together, these findings add a new layer to miRNA-mediated post-transcriptional gene regulation. In this newly emerging model, the cell-type-specific regulation of a target mRNA results from a 3′ UTR-encoded requirement for miRNA cooperation and an integration of partner miRNA availability within a critical time frame.

Materials and Methods

Mice

Tg(DO11.10); Tg(CARΔ-1) mice were obtained from Taconic Farms. Human CD2/CD52 Foxp3 reporter mice were kindly provided by Dr. S. Hori, RIKEN Institute, Japan. All animals were housed in a pathogen-free barrier facility in accordance with the Helmholtz Zentrum München and Ludwig-Maximilians-University institutional, state and federal guidelines. BALB/c.Thy1.1 × Dereg × DO11.10 and BALB/c.$Rag2^{-/-}$ mice were bred and maintained at the Experimental Center of the Medizinisch-Theoretisches Zentrum (TU Dresden, Germany) under specific pathogen-free conditions. Adoptive transfer and bone marrow reconstitution animal experiments were performed as approved by the Regieriungspräsidium Dresden and by the Regierung von Oberbayern, respectively.

Generation of adenoviral miRNA overexpression vectors and 3′ UTR reporter constructs

All primers used in this manuscript are listed in the Supplementary Materials. miRNA overexpression vectors were generated as described (Chen *et al*, 2004; Warth & Heissmeyer, 2013). Briefly, pri-miRNA sequences 250–500 nt up- and downstream of the mature miRNA or up to 1,000 nt up- and downstream of miRNA clusters were PCR-amplified and blunt end-ligated into the pENTR/D-TOPO vector (Life Technologies). miRNA inserts with wrong orientations were reverted through NotI/AscI restriction digests and subsequent ligation into a modified pENTR11 vector (Life

Technologies) containing NotI/AscI restriction sites. PCR fragments of the "pri-miR-451" that are positioned 5′ and 3′ of the mature miR-451 hairpin were generated by PCR using one primer each that overlapped by ~20 nt with the mature miR-451 hairpin sequence. For reprogramming, a synthetic oligonucleotide was used that encoded the mature 5p miRNA and a complementary sequence for hairpin formation, flanked by 19–21 nt of "pri-miR-451" 5′ or 3′ fragment sequence, as indicated in Fig 7A and the Supplementary Materials. This was added to a PCR mix with "pri-miR-451" 5′ and 3′ fragments together with "pri-miR-451" 5′ forward and "pri-miR-451" 3′ reverse primers (used for generation of the 5′ or 3′ fragments). In consecutive PCR rounds, the synthetic oligonucleotide 3′ overlapping sequence first serves as a primer on the 3′ "pri-miR-451" fragment for one cycle. The antisense sequence of the resulting product in turn serves as a primer on the "pri-miR-451" 5′ fragment (due to the 5′ overlapping sequences of the synthetic oligonucleotide) to generate the whole reprogrammed pri-miR-451 construct, which was then amplified by "pri-miR-451" 5′ forward and "pri-miR-451" 3′ reverse primers. The resulting PCR fragment was blunt end-cloned into the pENTR/D-TOPO entry vector. The "pri"-miRNA-sequence was then transferred into the pCAGAdDu adenoviral vector (Warth & Heissmeyer, 2013) using gateway recombination (Life Technologies).

Luciferase reporter constructs were generated by cloning PCR-amplified sequences of the Mtor 3′ UTR (1–825) into the pENTR/D-TOPO vector (Life Technologies). Gateway recombination was performed to transfer the respective DNA inserts into the pAdsi-CHECK vector, which is based on the pCAGAdDu vector, having the CAG-promoter-driven expression cassette replaced by the luciferase reporter cassette of the psiCHECK2 (Promega). This allows gateway recombination-dependent insertion of the 3′ UTR sequence downstream of the *Renilla* luciferase gene.

Mutated miRNA-binding sites in the *Mtor* 3′ UTR were generated using site-directed mutagenesis (QuikChange II, Agilent Technologies). Human FOXP3 expression constructs were previously described (Wu *et al*, 2006). For *cFos*-1-P2A-*cJun* expression vectors, the *cFos* open-reading frame was fused without Stop codon to a P2A-sequence, which connected to the *cJun* open-reading frame.

Antibodies and reagents

Hybridomas and monoclonal antibodies directed against panAgo (11G1) and Eri1 (5G8), polyclonal Eri1 (A28) as well as anti-CD3 (145-2C11), anti-CD28 (37N), anti-IL-12 (C17.8), anti-IL-4 (11B11) and anti-IFN-g (Xmg1.2) were produced in-house as previously described (Ansel *et al*, 2008; Glasmacher *et al*, 2010; Bronevetsky *et al*, 2013; Vogel *et al*, 2013). The polyclonal rabbit anti-mouse Foxp3 antibody was a kind gift from Steven F. Ziegler (Benaroya Research Institute, Seattle, USA). Anti-actin (I-19) and anti-tubulin (B-5-1-2) were obtained from Santa Cruz. Anti-mTOR (7C10) and anti-Iκbα (44D4) were obtained from Cell Signaling. Fluorescence-labeled anti-CD4 (GK1.5 or RM4-5), anti-CD5 (53-7.3), anti-CD25 (PC61.5), anti-CD44 (IM7), anti-CD62L (MEL-14), anti-CD69 (H1.2F3), anti-TCR-beta (H57-597), anti-DO11.10 (KJ1-26), anti-CD90.1 (Thy1.1, clone OX-7), anti-CD127 (A7R34), anti-IL-17A (eBio17B7), anti-Foxp3 (FJK16s), Fc receptor-blocking mAb against CD16/32 (93) and Pacific blue-conjugated streptavidin, as well as cell proliferation dye, were obtained from eBioscience or BD. LIVE/DEAD fixable dead cell stain kit was purchased from Life Technologies. Antagomirs were designed with the help of M-F. Mashreghi and were synthesized by Dharmacon/GE healthcare. Anti-mIL-2 (JES6-5H4) was purchased from Miltenyi Biotec. Recombinant mouse IL-6 or human TGFβ was purchased from R&D systems. Recombinant hIL-2 (ProleukinS) was obtained from Novartis. Phorbol-12-myristate-13-actetate (PMA) and ionomycin were purchased from Calbiochem. Brefeldin A and retinoic acid were purchased from Sigma-Aldrich.

Analysis of transcript variants

The Poly(A) sequencing data sets below generated by Derti *et al* (2012) were downloaded from http://www.ncbi.nlm.nih.gov/geo/ (study GSE30198) and analyzed using Integrative Genomics Viewer 2.3 (Broad Institute).
GSM747481_mouse_brain.sites.clustered.bed.gz,
GSM747482_mouse_kidney.alignments.sum.bed.gz,
GSM747482_mouse_kidney.sites.clustered.bed.gz,
GSM747483_mouse_liver.sites.clustered.bed.gz,
GSM747484_mouse_muscle.sites.clustered.bed.gz
GSM747485_mouse_testis.sites.clustered.bed.gz.

Cell isolation, infection, culture and stimulation

MEF cell lines were prepared and grown as previously described (Parameswaran *et al*, 2010). $Ago^{-/-}$ MEF cells were a kind gift of Gregory Hannon (CSHL Cold Spring Harbor, USA). Mouse spleens or lymph nodes were isolated and homogenized in a cell strainer. The solution was sieved through 70-μm fine mesh (Reichelt Chemietechnik), and the flow-through was used for the isolation of either naive $CD4^+$ T cells (Naive $CD4^+$ $CD62L^+$ T cell Isolation Kit II, mouse, Miltenyi Biotech) or $CD4^+$ T cells (Dynabeads Invitrogen), according to the manufacturers' instructions. T cells were cultured in RPMI cell culture medium, supplemented with 10% (vol/vol) FBS, 1× non-essential amino acids, 1 mM sodium pyruvate (Lonza), 10 mM HEPES pH 7.4, 1× eagle MEM essential vitamin mixture (Lonza), 2 mM L-glutamine (Invitrogen), 50 μM β-mercaptoethanol (Sigma) and 100 U/ml penicillin–streptomycin (Invitrogen) at 37°C in a humidified 10% CO_2 incubator. Naive $CD4^+$ T cells were stimulated in 96-well plates using an equal number of Dynabeads M-450 Tosylactivated (Life Technologies) pre-coupled to anti-CD3 (90 μm) and anti-CD28 (10 μm) per 4×10^8 beads. Purified $CD4^+$ T cells were stimulated on 6-well plates pre-coated overnight at 4°C with 50 mg/ml goat anti-hamster IgG (MP biochemicals) using anti-CD3 (0.5 μg/ml) and anti-CD28 (2.5 μg/ml). For Treg cell polarization, TGFβ (2 ng/ml) and IL-2 (100 U/ml) were added, and for Th17 cell polarization, TGFβ (2 ng/ml), IL-6 (5 ng/ml), anti-IL-12 (10 μg/ml), anti-IL-4 (10 μg/ml), anti-IFN-γ (5 μg/ml) and anti-IL-2 (2.5 μg/ml) were added and cells were cultured for 3 days. In Th17-polarizing conditions, cells were then restimulated for 5 h with PMA (20 nM) and ionomycin (1 μM) and adding brefeldin A (10 μg/ml) for the last 2.5 h prior to intracellular staining of the respective cytokines. After Treg polarization, cells were fixed and stained as previously described (Warth & Heissmeyer, 2013). Adenoviral infection of T cells, isolated from Tg(DO11.10); Tg(CARΔ-1) mice, was also performed as described (Warth & Heissmeyer, 2013). Briefly, cells were infected for 1.5 h at a multiplicity of infection MOI of 50–100 in 50 μl of T-cell medium. Cells were then washed in PBS and rested

for 4 h in culture medium at 37°C in a humidified 10% CO_2 incubator before stimulation. MEF cells were co-infected with reporter adenoviruses at an MOI of 20–100 and miRNA adenoviruses at an MOI of 100–1,000. The cells were cultured for 48 h before extraction and luciferase activity detection using the dual luciferase reporter kit (Promega).

Immunoblotting

For immunoblotting, the $CD4^+$ T cells were PBS-washed and incubated for 15 min on ice with lysis buffer (20 mM Tris–HCl, pH 7.5, 150 mM NaCl, 0.25% [vol/vol] Nonidet P-40, 1.5 mM $MgCl_2$, protease inhibitor mix without EDTA (Roche) and 1 mM DTT). After vortexing, the lysate was cleared by centrifugation (10 min, 10,000 × *g*, 4°C). The protein content in the lysate was determined using the Bradford protein quantification assay. For immunoblotting, 50–70 μg of total protein was loaded per lane and the detection was performed according to standard protocols.

Flow cytometry and intracellular staining

Single-cell suspensions were stained with fluorescence-labeled antibodies for 20 min on ice. For detection of intracellular cytokines, cells were stained with fixable dead cell staining solution (Invitrogen) for 30 min at 4°C. For Th17 staining, cells were then fixed with 4% paraformaldehyde (Merck) for 10 min at room temperature and permeabilized for 20 min at 4°C in PBS containing 0.5% saponin (VWR international) and 1% BSA (Roth). The cells were then stained with anti-IL-17A antibodies for 30 min at 4°C. For Treg staining, cells were fixed for 15 min in 2% paraformaldehyde (Merck) at room temperature, followed by a 30-min fixation and permeabilization period in 70% methanol on ice before washing and staining with anti-Foxp3 antibodies. For *in vivo* experiments, single-cell suspensions of spleen and pooled LNs (*Lnn. mesenterici, Lnn. mandibularis, Lnn. cervicales superficiales, Lnn. axillares et cubiti, Lnn. inguinales superficiales* and *Lnn. subiliaci*) were prepared using 70-μm cell strainers (BD). Before FACS sorting, $CD4^+$ cells were enriched from single-cell suspensions using biotinylated antibodies directed against CD4, streptavidin-conjugated microbeads and the AutoMACS magnetic separation system (Miltenyi Biotec). The acquisition was performed on an LSR Fortessa or LSR II (BD) device or sorted using an Aria II or III (BD), and the samples were analyzed with FlowJo software 9.5.2 (Tree Star).

Adoptive cell transfer

A total of 1×10^6 FACS-purified, $CD90.1^+CD4^+CD62L^+CD25^-$ $Foxp3(GFP)^-$ T cells were injected into the lateral tail veins of Thy1.2 BALB/c.$Rag2^{-/-}$ congenic recipient mice. After 14 days, cells were recovered from LNs and spleen of the recipients and analyzed by flow cytometry.

Lentiviral infection and bone marrow chimeras

Lentiviral vectors to express genes of interest in CD4/CD8 double-positive (DP) and in CD4 single-positive (CD4-SP) thymocytes were composed of CD4 regulatory elements previously described and kindly provided by Dr. David Klatzmann with the lentiviral vector backbone being provided by the laboratory of Dr. Brocker. Calcium phosphate transient transfection of 2×10^6 293FT cells was performed for lentivirus production. Mixture of 10 μg miR-expression vector with 8 μg pax2 DNA and 8 μg VSVg DNA was added to the cells. Lentiviral supernatants were collected at 18, 42 and 66 h after cotransfection, spun down at 38,000 *g* for 4 h, and aliquots were frozen at −80°C.

Bone marrow was obtained from femur and tibia bones of 10-week-old donor BALB/c mice harboring a human CD2 reporter transgene co-expressed from IRES sequences from the Foxp3 locus (Miyao *et al*, 2012). A single-cell solution was prepared, and donor T cells were depleted by using biotinylated anti-CD4 and anti-CD8 antibodies and streptavidin MACS beads (Miltenyi, Germany) according to the manufacturer's protocol. After depletion, bone marrow was plated out at 3×10^6 cells per infection. Infection was performed in Stemline medium (Sigma-Aldrich, Germany) supplemented with IL3 (20 ng/ml), IL6 (100 ng/ml) and SCF (50 ng/ml) (R&D Systems, Germany) at multiplicity of infection (MOI) of 1 for 6–8 h. After infection, cells were washed and injected intravenously in 2 × 450 rad irradiated, 8-week-old BALB/c mice. Chimeras were analyzed 8–10 weeks after reconstitution.

Quantitative real-time PCR

RNA was isolated from 1 to 5×10^6 activated T cells using 1 ml TRI Reagent (Sigma) or applying the miRNeasy Mini kit (Qiagen), according to manufacturer's instructions. RNA concentrations after resuspension in 25 μl RNase-free water ranged between 35–140 ng/μl for T cells and 75–450 ng/μl for MEF cells. For mRNA reverse transcription, 500 ng of RNA was used as template, and the reaction was performed using the Quantitect reverse transcription kit II (Qiagen), according to the manufacturer's instructions. The cDNA was diluted 1:5 in RNase-free water, and 5 μl of this dilution was used for each quantitative PCR. For miRNA-specific reverse transcription, 6 ng of RNA was used as template and the reaction was performed using the TaqMan MicroRNA reverse transcription kit and reverse transcription primers from the TaqMan MicroRNA Assays (Life Technologies), according to the manufacturer's instructions. Quantitative PCRs were performed in duplicates on 96-well PCR plates (4titude) using the Light Cycler 480 Probes Master kit (Roche). The assays were run on a Light Cycler 480II device with the Light Cycler 480 SW 1.5 software. The Cp values were determined using the second derivative maximum method, and the data were analyzed by advanced relative quantification. The transcripts were detected with the following forward and reverse primers as well as universal probes (Roche). Foxp3 (NM_001199347), Eri1 (NM_026067) CDS, Eri1 distal 3′ UTR and HPRT (NM_013556) were detected using oligonucleotides described in the Supplementary Materials. For detection of mature miRNAs and of the reference transcript snoRNA202, TaqMan MicroRNA Assays (Life Technologies) were used according to the manufacturer's instructions.

Statistical analysis

Statistical analysis was performed using GraphPad Prism 4.0 and 5.0 software, and *P*-values were calculated applying the Student's *t*-test or by one-way analysis of variance (ANOVA) followed by Tukey's multiple comparison test. Gaussian distribution of samples

was confirmed for all samples with $n > 4$. Asterisks: $^{*}P < 0.05$; $^{**}P < 0.01$; $^{***}P < 0.001$.

Supplementary information for this article is available online: http://emboj.embopress.org

Acknowledgements

We thank Christine Federle, Ariya D. Lapan, Christine Wolf, Lirui Du and Young Minh Moon for technical assistance or help on establishing biochemical assays or adenoviral transduction. We are grateful to Drs. Mir-Fazin Mashreghi and Andreas Radbruch for advice on the use of antagomirs. This work was supported by grants from the DFG (SFB1054 TP-A03 and Z2 to VH and TP-A01 to LK) and by the European Commission through a European Research Council Grant to VH.

Author contributions

SCW performed most of the experiments and together with AH constructed the adenoviral miRNA library. Bone marrow chimera and adoptive transfer experiments were performed by KJ and SS, respectively. KPH contributed some experiments. VH conceived and initiated the project with critical input from KMA, LK and KK, and VH and SCW designed the experiments and wrote the paper together with KPH.

Conflict of interest

The authors declare that they have no conflict of interest.

References

Ansel KM, Pastor WA, Rath N, Lapan AD, Glasmacher E, Wolf C, Smith LC, Papadopoulou N, Lamperti ED, Tahiliani M, Ellwart JW, Shi Y, Kremmer E, Rao A, Heissmeyer V (2008) Mouse Eri1 interacts with the ribosome and catalyzes 5.8S rRNA processing. *Nat Struct Mol Biol* 15: 523 – 530

Baumjohann D, Kageyama R, Clingan JM, Morar MM, Patel S, de Kouchkovsky D, Bannard O, Bluestone JA, Matloubian M, Ansel KM, Jeker LT (2013) The microRNA cluster miR-17~92 promotes TFH cell differentiation and represses subset-inappropriate gene expression. *Nat Immunol* 8: 840 – 848

Bettelli E, Carrier Y, Gao W, Korn T, Strom TB, Oukka M, Weiner HL, Kuchroo VK (2006) Reciprocal developmental pathways for the generation of pathogenic effector TH17 and regulatory T cells. *Nature* 441: 235 – 238

Broderick JA, Salomon WE, Ryder SP, Aronin N, Zamore PD (2011) Argonaute protein identity and pairing geometry determine cooperativity in mammalian RNA silencing. *RNA* 17: 1858 – 1869

Bronevetsky Y, Villarino AV, Eisley CJ, Barbeau R, Barczak AJ, Heinz GA, Kremmer E, Heissmeyer V, McManus MT, Erle DJ, Rao A, Ansel KM (2013) T cell activation induces proteasomal degradation of Argonaute and rapid remodeling of the microRNA repertoire. *J Exp Med* 210: 417 – 432

Chen W, Jin W, Hardegen N, Lei K-J, Li L, Marinos N, McGrady G, Wahl SM (2003) Conversion of peripheral $CD4^{+}CD25^{-}$ naive T cells to $CD4^{+}CD25^{+}$ regulatory T cells by TGF-beta induction of transcription factor Foxp3. *J Exp Med* 198: 1875 – 1886

Chen C-Z, Li L, Lodish HF, Bartel DP (2004) MicroRNAs modulate hematopoietic lineage differentiation. *Science* 303: 83 – 86

Chong MMW, Rasmussen JP, Rudensky AY, Littman DR (2008) The RNAseIII enzyme Drosha is critical in T cells for preventing lethal inflammatory disease. *J Exp Med* 205: 2005 – 2017

Cifuentes D, Xue H, Taylor DW, Patnode H, Mishima Y, Cheloufi S, Ma E, Mane S, Hannon GJ, Lawson ND, Wolfe SA, Giraldez AJ (2010) A novel miRNA processing pathway independent of Dicer requires Argonaute2 catalytic activity. *Science* 328: 1694 – 1698

Cobb BS, Hertweck A, Smith J, O'Connor E, Graf D, Cook T, Smale ST, Sakaguchi S, Livesey FJ, Fisher AG, Merkenschlager M (2006) A role for Dicer in immune regulation. *J Exp Med* 203: 2519 – 2527

Dang EV, Barbi J, Yang H-Y, Jinasena D, Yu H, Zheng Y, Bordman Z, Fu J, Kim Y, Yen H-R, Luo W, Zeller K, Shimoda L, Topalian SL, Semenza GL, Dang CV, Pardoll DM, Pan F (2011) Control of T(H)17/T(reg) balance by hypoxia-inducible factor 1. *Cell* 146: 772 – 784

De Kouchkovsky D, Esensten JH, Rosenthal WL, Morar MM, Bluestone JA, Jeker LT (2013) microRNA-17-92 regulates IL-10 production by regulatory T cells and control of experimental autoimmune encephalomyelitis. *J Immunol* 191: 1594 – 1605

Delgoffe GM, Kole TP, Zheng Y, Zarek PE, Matthews KL, Xiao B, Worley PF, Kozma SC, Powell JD (2009) The mTOR kinase differentially regulates effector and regulatory T cell lineage commitment. *Immunity* 30: 832 – 844

Derti A, Garrett-Engele P, Macisaac KD, Stevens RC, Sriram S, Chen R, Rohl CA, Johnson JM, Babak T (2012) A quantitative atlas of polyadenylation in five mammals. *Genome Res* 22: 1173 – 1183

Diederichs S, Haber DA (2007) Dual role for argonautes in microRNA processing and posttranscriptional regulation of microRNA expression. *Cell* 131: 1097 – 1108

Du C, Liu C, Kang J, Zhao G, Ye Z, Huang S, Li Z, Wu Z, Pei G (2009) MicroRNA miR-326 regulates TH-17 differentiation and is associated with the pathogenesis of multiple sclerosis. *Nat Immunol* 10: 1252 – 1259

Dueck A, Ziegler C, Eichner A, Berezikov E, Meister G (2012) microRNAs associated with the different human Argonaute proteins. *Nucleic Acids Res* 40: 9850 – 9862

Foley NH, Bray I, Watters KM, Das S, Bryan K, Bernas T, Prehn JHM, Stallings RL (2011) MicroRNAs 10a and 10b are potent inducers of neuroblastoma cell differentiation through targeting of nuclear receptor corepressor 2. *Cell Death Differ* 18: 1089 – 1098

Fontenot JD, Gavin Ma, Rudensky AY (2003) Foxp3 programs the development and function of $CD4^{+}CD25^{+}$ regulatory T cells. *Nat Immunol* 4: 330 – 336

Glasmacher E, Hoefig KP, Vogel KU, Rath N, Du L, Wolf C, Kremmer E, Wang X, Heissmeyer V (2010) Roquin binds inducible costimulator mRNA and effectors of mRNA decay to induce microRNA-independent post-transcriptional repression. *Nat Immunol* 11: 725 – 733

Grimson A, Farh KK-H, Johnston WK, Garrett-Engele P, Lim LP, Bartel DP (2007) MicroRNA targeting specificity in mammals: determinants beyond seed pairing. *Mol Cell* 27: 91 – 105

Hori S, Nomura T, Sakaguchi S (2003) Control of regulatory T cell development by the transcription factor Foxp3. *Science* 299: 1057 – 1061

Jeker LT, Zhou X, Gershberg K, de Kouchkovsky D, Morar MM, Stadthagen G, Lund AH, Bluestone JA (2012) MicroRNA 10a marks regulatory T cells. *PLoS ONE* 7: e36684

Jiang S, Li C, Olive V, Lykken E, Feng F, Sevilla J, Wan Y, He L, Li Q-J (2011) Molecular dissection of the miR-17-92 cluster's critical dual roles in promoting Th1 responses and preventing inducible Treg differentiation. *Blood* 118: 5487 – 5497

Jordan MS, Boesteanu A, Reed AJ, Petrone AL, Holenbeck AE, Lerman MA, Naji A, Caton AJ (2001) Thymic selection of $CD4^{+}CD25^{+}$ regulatory T cells induced by an agonist self-peptide. *Nat Immunol* 2: 301 – 306

Josefowicz SZ, Niec RE, Kim HY, Treuting P, Chinen T, Zheng Y, Umetsu DT, Rudensky AY (2012) Extrathymically generated regulatory T cells control mucosal TH2 inflammation. *Nature* 482: 395 – 399

Kang SG, Liu W-H, Lu P, Jin HY, Lim HW, Shepherd J, Fremgen D, Verdin E, Oldstone MBA, Qi H, Teijaro JR, Xiao C (2013) MicroRNAs of the miR-17~92

family are critical regulators of TFH differentiation. *Nat Immunol* 14: 849 – 857

Kretschmer K, Apostolou I, Hawiger D, Khazaie K, Nussenzweig MC, von Boehmer H (2005) Inducing and expanding regulatory T cell populations by foreign antigen. *Nat Immunol* 6: 1219 – 1227

Krützfeldt J, Rajewsky N, Braich R, Rajeev KG, Tuschl T, Manoharan M, Stoffel M (2005) Silencing of microRNAs *in vivo* with "antagomirs". *Nature* 438: 685 – 689

Landgraf P, Rusu M, Sheridan R, Sewer A, Iovino N, Aravin A, Pfeffer S, Rice A, Kamphorst AO, Landthaler M, Lin C, Socci ND, Hermida L, Fulci V, Chiaretti S, Foà R, Schliwka J, Fuchs U, Novosel A, Müller R-U *et al* (2007) A mammalian microRNA expression atlas based on small RNA library sequencing. *Cell* 129: 1401 – 1414

Liston A, Lu L-F, O'Carroll D, Tarakhovsky A, Rudensky AY (2008) Dicer-dependent microRNA pathway safeguards regulatory T cell function. *J Exp Med* 205: 1993 – 2004

Liu J (2009) Calmodulin-dependent phosphatase, kinases, and transcriptional corepressors involved in T-cell activation. *Immunol Rev* 228: 184 – 198

Liu S-Q, Jiang S, Li C, Zhang B, Li Q-J (2014) miR-17-92 cluster targets phosphatase and tensin homology and Ikaros family Zinc finger 4 to promote TH17-mediated inflammation. *J Biol Chem* 289: 12446 – 12456

Lu L-F, Thai T-H, Calado DP, Chaudhry A, Kubo M, Tanaka K, Loeb GB, Lee H, Yoshimura A, Rajewsky K, Rudensky AY (2009) Foxp3-dependent microRNA155 confers competitive fitness to regulatory T cells by targeting SOCS1 protein. *Immunity* 30: 80 – 91

Lu L-F, Boldin MP, Chaudhry A, Lin L-L, Taganov KD, Hanada T, Yoshimura A, Baltimore D, Rudensky AY (2010) Function of miR-146a in controlling Treg cell-mediated regulation of Th1 responses. *Cell* 142: 914 – 929

Meseguer S, Mudduluru G, Escamilla JM, Allgayer H, Barettino D (2011) MicroRNAs-10a and -10b contribute to retinoic acid-induced differentiation of neuroblastoma cells and target the alternative splicing regulatory factor SFRS1 (SF2/ASF). *J Biol Chem* 286: 4150 – 4164

Miyao T, Floess S, Setoguchi R, Luche H, Fehling HJ, Waldmann H, Huehn J, Hori S (2012) Plasticity of Foxp3(+) T cells reflects promiscuous Foxp3 expression in conventional T cells but not reprogramming of regulatory T cells. *Immunity* 36: 262 – 275

Monticelli S, Ansel KM, Xiao C, Socci ND, Krichevsky AM, Thai T-H, Rajewsky N, Marks DS, Sander C, Rajewsky K, Rao A, Kosik KS (2005) MicroRNA profiling of the murine hematopoietic system. *Genome Biol* 6: 1 – 15

Mucida D, Park Y, Kim G, Turovskaya O, Scott I, Kronenberg M, Cheroutre H (2007) Reciprocal TH17 and regulatory T cell differentiation mediated by retinoic acid. *Science* 317: 256 – 260

Mueller AC, Sun D, Dutta A (2012) The miR-99 family regulates the DNA damage response through its target SNF2H. *Oncogene* 32: 1164 – 1172

Muljo SA, Ansel KM, Kanellopoulou C, Livingston DM, Rao A, Rajewsky K (2005) Aberrant T cell differentiation in the absence of Dicer. *J Exp Med* 202: 261 – 269

Nagaraja AK, Creighton CJ, Yu Z, Zhu H, Gunaratne PH, Reid JG, Olokpa E, Itamochi H, Ueno NT, Hawkins SM, Anderson ML, Matzuk MM (2010) A link between mir-100 and FRAP1/mTOR in clear cell ovarian cancer. *Mol Endocrinol* 24: 447 – 463

Nolting J, Daniel C, Reuter S, Stuelten C, Li P, Sucov H, Kim B-G, Letterio JJ, Kretschmer K, Kim H-J, Von Boehmer H (2009) Retinoic acid can enhance conversion of naive into regulatory T cells independently of secreted cytokines. *J Exp Med* 206: 2131 – 2139

O'Carroll D, Mecklenbrauker I, Das PP, Santana A, Koenig U, Enright AJ, Miska EA, Tarakhovsky A (2007) A slicer-independent role for Argonaute 2 in hematopoiesis and the microRNA pathway. *Genes Dev* 21: 1999 – 2004

O'Connell RM, Kahn D, Gibson WSJ, Round JL, Scholz RL, Chaudhuri AA, Kahn ME, Rao DS, Baltimore D (2010) MicroRNA-155 promotes autoimmune inflammation by enhancing inflammatory T cell development. *Immunity* 33: 607 – 619

Oneyama C, Ikeda J, Okuzaki D, Suzuki K, Kanou T, Shintani Y, Morii E, Okumura M, Aozasa K, Okada M (2011) MicroRNA-mediated downregulation of mTOR/FGFR3 controls tumor growth induced by Src-related oncogenic pathways. *Oncogene* 30: 3489 – 3501

Parameswaran P, Sklan E, Wilkins C, Burgon T, Samuel Ma, Lu R, Ansel KM, Heissmeyer V, Einav S, Jackson W, Doukas T, Paranjape S, Polacek C, dos Santos FB, Jalili R, Babrzadeh F, Gharizadeh B, Grimm D, Kay M, Koike S *et al* (2010) Six RNA viruses and forty-one hosts: viral small RNAs and modulation of small RNA repertoires in vertebrate and invertebrate systems. *PLoS Pathog* 6: e1000764

Rouas R, Fayyad-Kazan H, El Zein N, Lewalle P, Rothé F, Simion A, Akl H, Mourtada M, El Rifai M, Burny A, Romero P, Martiat P, Badran B (2009) Human natural Treg microRNA signature: role of microRNA-31 and microRNA-21 in FOXP3 expression. *Eur J Immunol* 39: 1608 – 1618

Sætrom P, Heale BSE, Snøve O, Aagaard L, Alluin J, Rossi JJ (2007) Distance constraints between microRNA target sites dictate efficacy and cooperativity. *Nucleic Acids Res* 35: 2333 – 2342

Samstein RM, Josefowicz SZ, Arvey A, Treuting PM, Rudensky AY (2012) Extrathymic generation of regulatory T cells in placental mammals mitigates maternal-fetal conflict. *Cell* 150: 29 – 38

Sandberg R, Neilson JR, Sarma A, Sharp PA, Burge CB (2008) Proliferating cells express mRNAs with shortened 3′ untranslated regions and fewer microRNA target sites. *Science* 320: 1643 – 1647

Shevach EM, Thornton AM (2014) tTregs, pTregs, and iTregs: similarities and differences. *Immunol Rev* 259: 88 – 102

Shi LZ, Wang R, Huang G, Vogel P, Neale G, Green DR, Chi H (2011) HIF1alpha-dependent glycolytic pathway orchestrates a metabolic checkpoint for the differentiation of TH17 and Treg cells. *J Exp Med* 208: 1367 – 1376

Sledzińska A, Hemmers S, Mair F, Gorka O, Ruland J, Fairbairn L, Nissler A, Müller W, Waisman A, Becher B, Buch T (2013) TGF-β signalling is required for $CD4^+$ T cell homeostasis but dispensable for regulatory T cell function. *PLoS Biol* 11: e1001674

Steiner DF, Thomas MF, Hu JK, Yang Z, Babiarz JE, Allen CDC, Matloubian M, Blelloch R, Ansel KM (2011) MicroRNA-29 regulates T-box transcription factors and interferon-γ production in helper T cells. *Immunity* 35: 169 – 181

Stittrich AB, Haftmann C, Sgouroudis E, Kühl AA, Hegazy AN, Panse I, Riedel R, Flossdorf M, Dong J, Fuhrmann F, Heinz GA, Fang Z, Li N, Bissels U, Hatam F, Jahn A, Hammoud B, Matz M, Schulze FM, Baumgrass R *et al* (2010) The microRNA miR-182 is induced by IL-2 and promotes clonal expansion of activated helper T lymphocytes. *Nat Immunol* 11: 1057 – 1062

Takahashi H, Kanno T, Nakayamada S, Hirahara K, Sciumè G, Muljo SA, Kuchen S, Casellas R, Wei L, Kanno Y, O'Shea JJ (2012) TGF-β and retinoic acid induce the microRNA miR-10a, which targets Bcl-6 and constrains the plasticity of helper T cells. *Nat Immunol* 13: 587 – 595

Thomas MF, Abdul-Wajid S, Panduro M, Babiarz JE, Rajaram M, Woodruff P, Lanier LL, Heissmeyer V, Ansel KM (2012) Eri1 regulates microRNA homeostasis and mouse lymphocyte development and antiviral function. *Blood* 120: 130 – 142

Torres A, Torres K, Pesci A, Ceccaroni M, Paszkowski T, Cassandrini P, Zamboni G, Maciejewski R (2012) Deregulation of miR-100, miR-99a and miR-199b in tissues and plasma coexists with increased expression of mTOR kinase in endometrioid endometrial carcinoma. *BMC Cancer* 12: 369

Veldhoen M, Hocking RJ, Atkins CJ, Locksley RM, Stockinger B (2006) TGFbeta in the context of an inflammatory cytokine milieu supports *de novo* differentiation of IL-17-producing T cells. *Immunity* 24: 179 – 189

Vogel KU, Edelmann SL, Jeltsch KM, Bertossi A, Heger K, Heinz GA, Zöller J, Warth SC, Hoefig KP, Lohs C, Neff F, Kremmer E, Schick J, Repsilber D, Geerlof A, Blum H, Wurst W, Heikenwälder M, Schmidt-Supprian M, Heissmeyer V (2013) Roquin paralogs 1 and 2 redundantly repress the Icos and Ox40 costimulator mRNAs and control follicular helper T cell differentiation. *Immunity* 38: 655 – 668

Wan YY, Leon RP, Marks R, Cham CM, Schaack J, Gajewski TF, DeGregori J (2000) Transgenic expression of the coxsackie/adenovirus receptor enables adenoviral-mediated gene delivery in naive T cells. *Proc Natl Acad Sci USA* 97: 13784 – 13789

Wan Y, Qu K, Zhang QC, Flynn Ra, Manor O, Ouyang Z, Zhang J, Spitale RC, Snyder MP, Segal E, Chang HY (2014) Landscape and variation of RNA secondary structure across the human transcriptome. *Nature* 505: 706 – 709

Warth SC, Heissmeyer V (2013) Adenoviral transduction of naive CD4 T cells to study treg differentiation. *J Vis Exp* 78: e50455

Wu Y, Borde M, Heissmeyer V, Feuerer M, Lapan AD, Stroud JC, Bates DL, Guo L, Han A, Ziegler SF, Mathis D, Benoist C, Chen L, Rao A (2006) FOXP3 controls regulatory T cell function through cooperation with NFAT. *Cell* 126: 375 – 387

Yang XO, Nurieva R, Martinez GJ, Kang HS, Chung Y, Pappu BP, Shah B, Chang SH, Schluns KS, Watowich SS, Feng X-H, Jetten AM, Dong C (2008a) Molecular antagonism and plasticity of regulatory and inflammatory T cell programs. *Immunity* 29: 44 – 56

Yang XO, Pappu BP, Nurieva R, Akimzhanov A, Kang HS, Chung Y, Ma L, Shah B, Panopoulos AD, Schluns KS, Watowich SS, Tian Q, Jetten AM, Dong C (2008b) T helper 17 lineage differentiation is programmed by orphan nuclear receptors ROR alpha and ROR gamma. *Immunity* 28: 29 – 39

Yang J-S, Maurin T, Robine N, Rasmussen KD, Jeffrey KL, Chandwani R, Papapetrou EP, Sadelain M, O'Carroll D, Lai EC (2010) Conserved vertebrate mir-451 provides a platform for Dicer-independent, Ago2-mediated microRNA biogenesis. *Proc Natl Acad Sci USA* 107: 15163 – 15168

Yang J-S, Maurin T, Lai EC (2012) Functional parameters of Dicer-independent microRNA biogenesis. *RNA* 18: 945 – 957

Yoda M, Cifuentes D, Izumi N, Sakaguchi Y, Suzuki T, Giraldez AJ, Tomari Y (2013) Poly(A)-specific ribonuclease mediates 3′-end trimming of argonaute2-cleaved precursor microrna. *Cell Rep* 5: 715 – 726

Zhang X, Izikson L, Liu L, Weiner HL (2001) Activation of CD25(+)CD4(+) regulatory T cells by oral antigen administration. *J Immunol* 167: 4245 – 4253

Zheng SG, Wang JH, Koss MN, Quismorio F, Gray JD, Horwitz DA (2004) $CD4^+$ and $CD8^+$ regulatory T cells generated *ex vivo* with IL-2 and TGF-beta suppress a stimulatory graft-versus-host disease with a lupus-like syndrome. *J Immunol* 172: 1531 – 1539

Zhou L, Lopes JE, Chong MMW, Ivanov II, Min R, Victora GD, Shen Y, Du J, Rubtsov YP, Rudensky AY, Ziegler SF, Littman DR (2008a) TGF-beta-induced Foxp3 inhibits T(H)17 cell differentiation by antagonizing RORgammat function. *Nature* 453: 236 – 240

Zhou X, Jeker LT, Fife BT, Zhu S, Anderson MS, McManus MT, Bluestone JA (2008b) Selective miRNA disruption in T reg cells leads to uncontrolled autoimmunity. *J Exp Med* 205: 1983 – 1991

Zhou H, Huang X, Cui H, Luo X, Tang Y, Chen S, Wu L, Shen N (2010) miR-155 and its star-form partner miR-155* cooperatively regulate type I interferon production by human plasmacytoid dendritic cells. *Blood* 116: 5885 – 5894